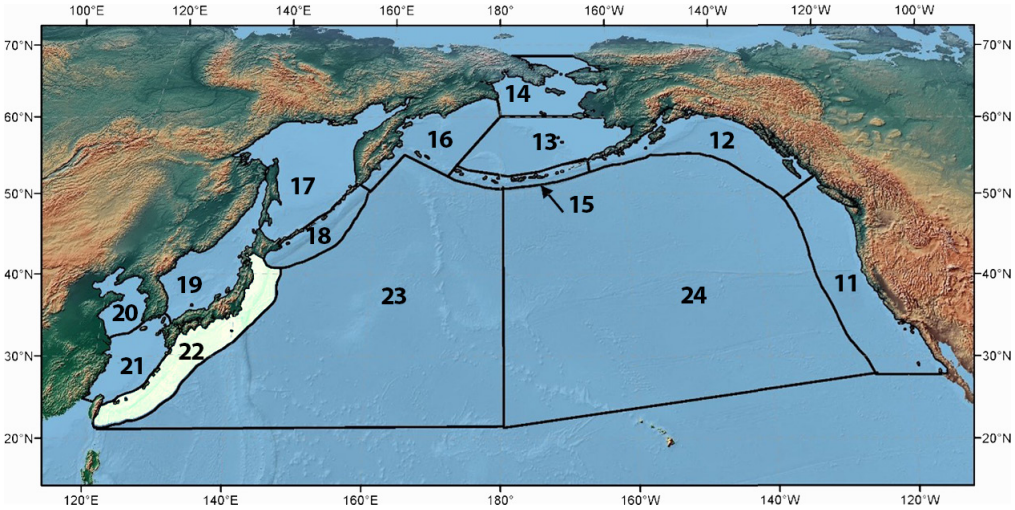

PICES

Regional Report for PICES Region: 22

PICES SPECIAL PUBLICATION 7

Marine Ecosystems of the North Pacific Ocean 2009–2016

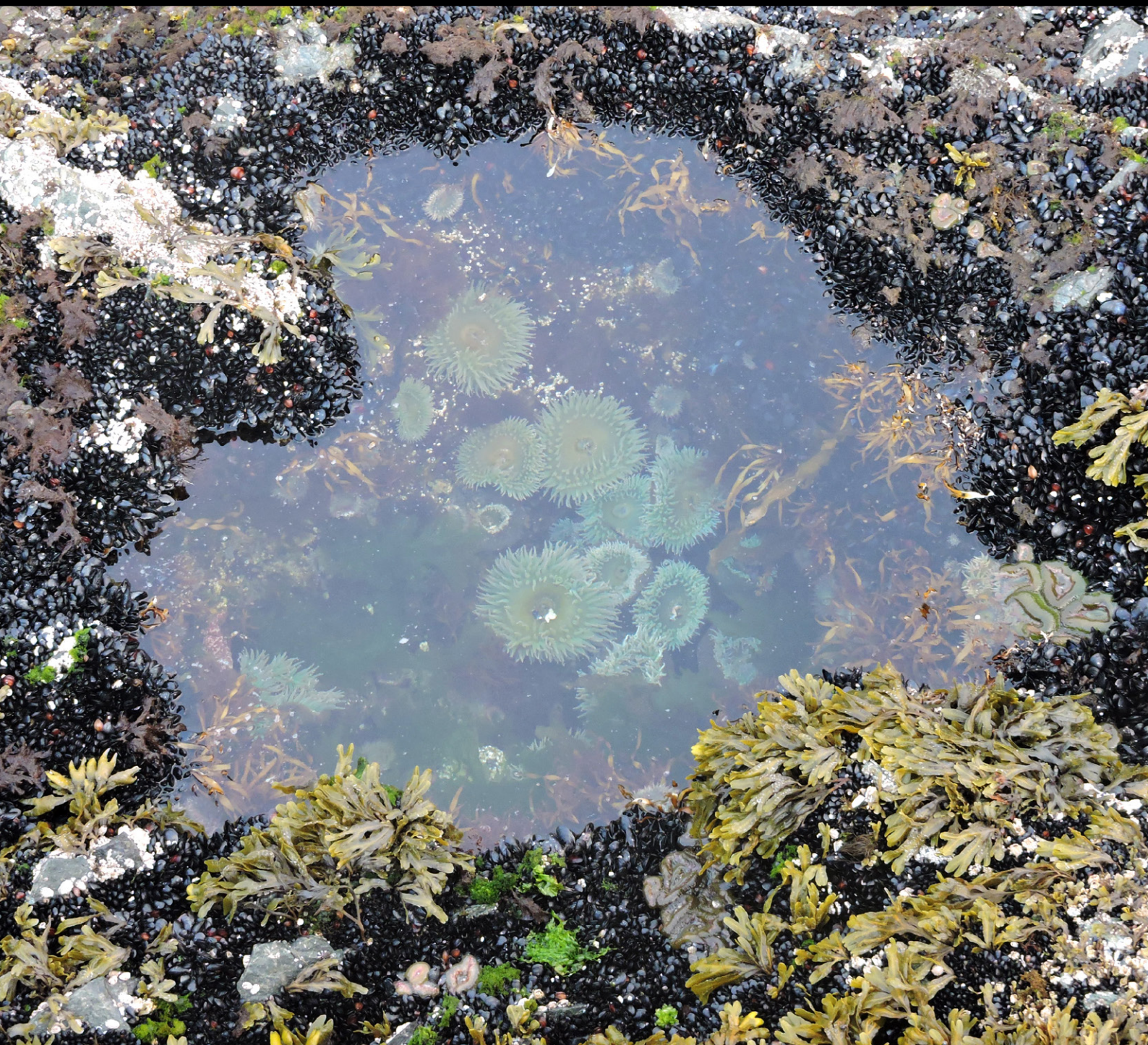

PICES North Pacific Ecosystem Status Report, Region 22 (Kuroshio)

Kazuaki Tadokoro
Fisheries Resources Institute (Shiogama)
Japan Fisheries Research and Education Agency (FRA)
Miyagi, Japan

Contributors:

Kityotaka Hidaka[1],Takeshi Okunishi[1], Tsuneo Ono[1], Yoshioki Oozeki[2], Chiyuki Sassa[1], Takashi Setou[1], Yugo Shimizu[3], Shusaku Sugimoto[4], Akinori Takasuka[5], Keiichi Yamazaki[6]

[1]Fisheries Resources Institute, Japan Fisheries Research and Education Agency
[2]Japan Fisheries Research and Education Agency
[3]Fisheries Agency, Japan
[4]Graduate School of Science, Tohoku University
[5]Graduate School of Agricultural and Life Sciences, The University of Tokyo
[6]Japan Marine Fisheries Research and Development Center, Japan Fisheries Research and Education Agency

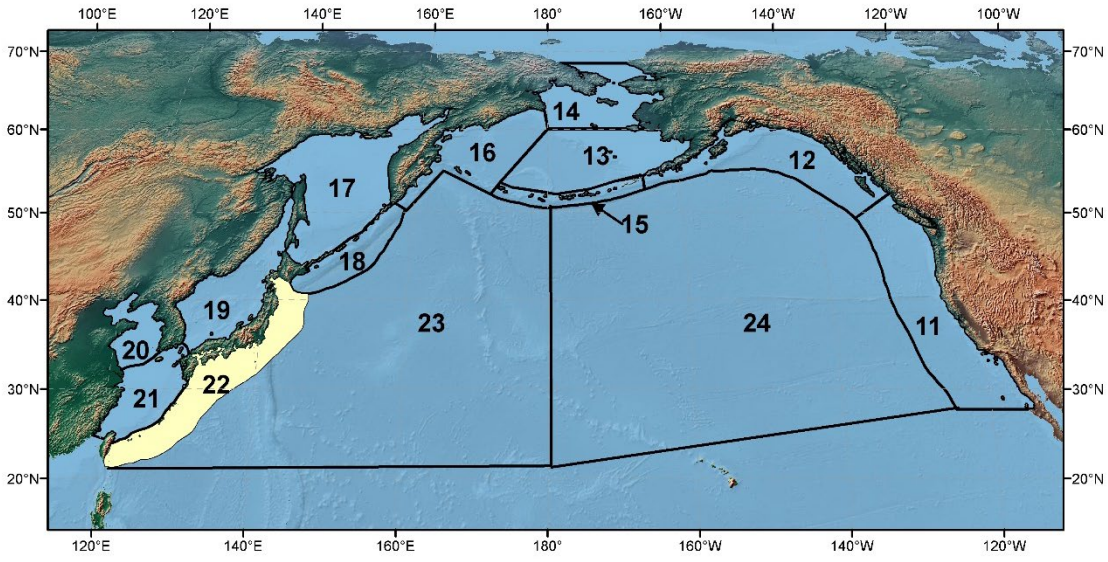

Figure R22-1. The PICES biogeographical regions and naming convention for the North Pacific Ocean with the area discussed in this report highlighted.

1. Highlights

- Sea surface temperature in the Kuroshio represented significant increase trends from 1982 to 2012, and the most intense warming is seen in the Kuroshio current area.
- Depth of the nutricline showed a significant deepening trend after 2010 in the slope area of the Kuroshio, and a negative correlation with total N concentration. This suggests that the surface concentration of winter nitrate is mainly controlled by the depth of the nutricline.
- In the eastern area, the copepod biomass remained stable in 2004–2010 and a large biomass was observed after 2011. On the other hand, a large copepod biomass was seen in 2003, 2007 and 2008 in the western area.
- Recently, Japanese sardine populations have started to increase, showing a sign of their population recovery. In contrast, the population levels of anchovy, jack mackerel, and common squid are now declining simultaneously.

2. Introduction

The Kuroshio originating in the North Equatorial Current, is one of the strongest western boundary currents in the World Ocean. It flows along the south side of the Japanese Archipelago, crossing three shallow ridges – one east of Taiwan, through Tokara Strait, and across the Izu-Ogasawara ridges. The width of the Kuroshio is about 100 km and has a current speed of 1-2 $m \cdot s^{-1}$. The depth of the current axis is usually >500 m and the transport volume is about 50 Sv. It transports a large volume of water and heat from south to north, and affects the climate and oceanographic conditions in the North Pacific Ocean. It also forms sub-meso and meso scale eddies around the current axis. Recent studies suggest that the eddies affect the important role of nutrient conditions and marine ecosystems. Moreover, the Kuroshio transports marine organisms from south to north of the North Pacific Ocean. Many species of pelagic fishes such as Japanese sardine (*Sardinops melanostictus*) and Pacific saury (*Cololabis saira*) utilize the current for early stage migration. The conditions of the Kuroshio have varied due to, e.g., the Pacific Decadal Oscillation and global warming, and these changes are considered to affect the marine ecosystems and fish stocks. This report contains a review of the status and trends of the Kuroshio Region from 2006–2016, hereafter termed the focus period.

3. Atmosphere

(Shusaku Sugimoto)

Over the last 10 years, the accumulation of satellite-derived altimeter sea surface height (SSH) data and advancements in eddy-resolving ocean general circulation models have revealed variabilities in the Kuroshio and Kuroshio Extension (KE) paths (Figure R22-2a) on a low-frequency timescale. Concurrently, developments in assimilation technology and regional atmospheric models have provided new perspectives on the influence of the Kuroshio/KE on the overlying atmosphere.

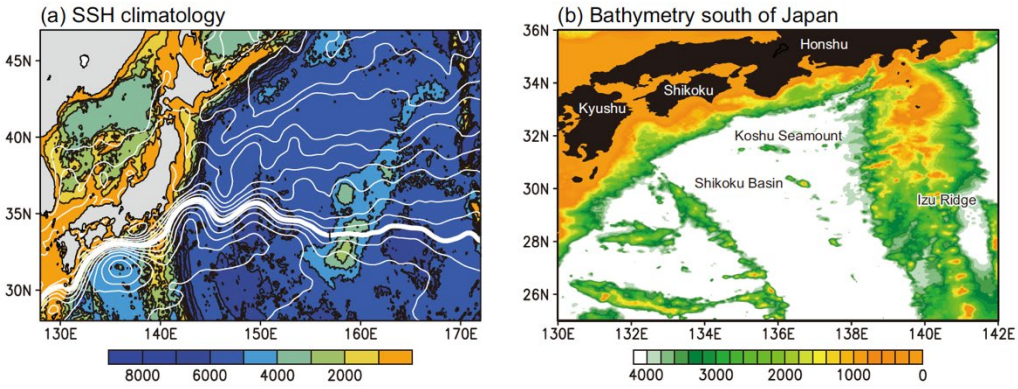

Figure R22-2. (a) Climatological SSH field (1993–2016) reconstructed from satellite-derived altimetry SSH anomaly data and mean dynamic topography data, by the Copernicus Marine and Environment Monitoring Service (CMEMS) (http://www.marine.copernicus.eu). Contour interval is 0.1 m. Thick white line indicates the axis of the Kuroshio and KE, which is defined as the 1.0 m SSH isoline. Shading represents the bathymetry features based on the National Geophysical Data Center's 2-min global relief data (ETOPO2, NGDC 2006) (m). (b) Bathymetry features (m) south of Japan.

3.1. Influence of the Kuroshio south of Japan on the atmosphere

3.1.1. Climatological features

The Kuroshio brings large amounts of warm water in the low-latitude to mid-latitude ocean. In the region south of Japan, the warm surface water of the Kuroshio releases a vigorous amount of heat in the form of sensible and latent heat fluxes (SHF and LHF) to the atmosphere under the winter monsoon with cold and dry continental air. The wintertime turbulent heat flux (THF; sum of SHF and LHF) over the Kuroshio south of Japan reaches about 500 W m^{-2} (Figure R22-3a).

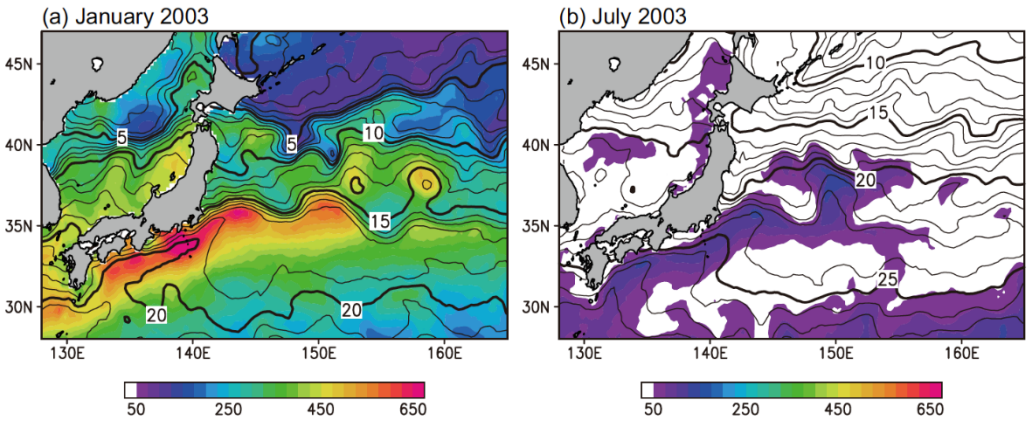

Figure R22-3. Upward THF (W m^{-2}) from the Japanese Ocean Flux Data Sets with Use of Remote Sensing Observations version 3 (J-OFURO3) (https://j-ofuro.isee.nagoya-u.ac.jp/en/) (shading), (a) January 2003 and (b) July 2003. Contours represent SST with an interval of 1°C, from the J-OFURO3.

Over the extratropical ocean, surface winds generally enhance upward heat release from the ocean to the atmosphere (Davis 1976; Frankignoul 1985; Iwasaka et al., 1987; Frankignoul and Kestenare 2002), resulting in a cold ocean surface where sea surface temperature (SST) is negatively correlated with surface winds. However, high-resolution satellite measurements have indicated that surface wind speed increases over the warm Kuroshio (e.g., Nonaka and Xie 2003) (Figure R22-4), resulting in a positive correlation between SST and surface winds over the Kuroshio. This in-phase relationship between SST and surface winds is in contrast to the traditional view that strong wind speed cools the surface ocean, and strongly suggests an active role of the Kuroshio on the regional atmospheric and climate systems (Kwon et al., 2010).

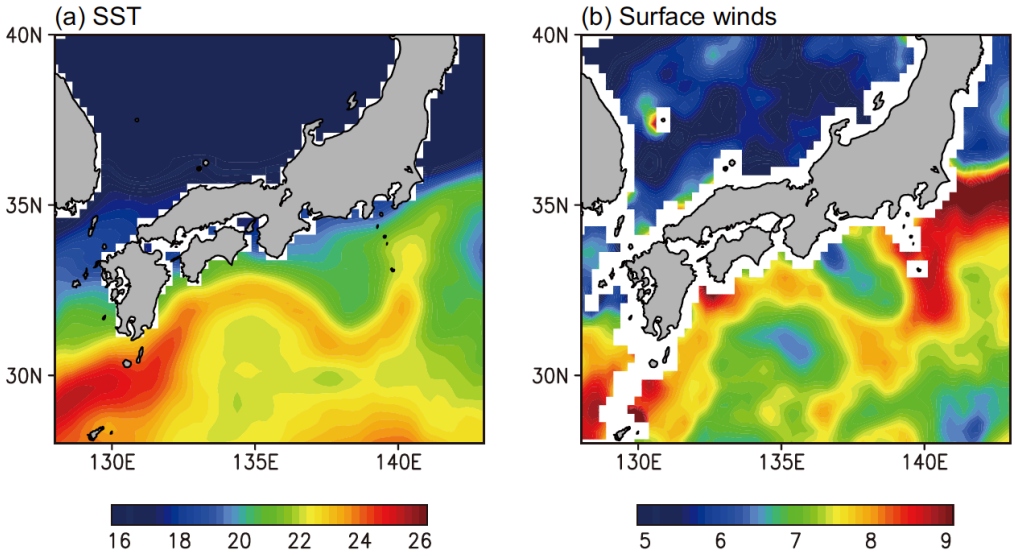

Figure R22-4. (a) SST (°C) from the NOAA Optimum Interpolation SST (OISST) (Reynolds et al., 2007) and (b) surface wind speed (m s^{-1}) from the QuikSCAT product, in May 2005.

3.1.2. Decadal-scale variability of the Kuroshio paths

The Kuroshio south of Japan has two main paths, the large meander (LM) path and the straight path. These two paths can persist for anywhere from a year to a decade (Kawabe 1987). Recent studies reported that the LM path tends to occur and persist when the volume transport is low (Tsujino et al., 2013; Usui et al., 2013) and that enhanced baroclinic instability over the northern slope of the Koshu Seamount is a prerequisite for the occurrence of the LM (Endoh and Hibiya 2001; Endoh et al., 2011). It is notable that the last LM event occurred in 2004–2005, and it has not occurred in the 13 years since.

Under the LM path, a local recirculation develops in the Shikoku Basin, leading to a warm SST pool south of the Kuroshio (Sugimoto and Hanawa 2012). An increase in horizontal heat advection due to the westward flow associated with this local recirculation causes surface ocean warming in the Shikoku Basin, leading to an enhanced upward THF with warm SST in the basin. A cold SST pool appears between the Pacific side of Honshu (the main island of Japan) and the Kuroshio (e.g., Fig. R22-3a) during the LM path, suppressing upward heat release from the ocean to the atmosphere and decreasing surface wind speed, through both the vertical mixing effects of wind momentum and pressure adjustment process (Xu et al., 2010; Murazaki et al., 2015). In summer, the deceleration of surface winds over the cold SST pool

represents a local weakening of the southerly monsoon. This atmospheric response results in a decrease in the transport of water vapor, a greenhouse gas, from the Pacific Ocean to Honshu, leading to cold summers over the Pacific coast of Honshu (Takahashi et al., 2015). When the Kuroshio takes the LM path, the wintertime extratropical cyclone track passing over the south of Japan tends to shift southward slightly (Nakamura et al., 2012; Hayasaki et al., 2013) , which causes a decrease in air temperature and heavy snowfall in Tokyo (Nakamura et al., 2012). This southward shift of cyclones might be due to suppressed upward heat release over the cold pool between the Pacific coast of Honshu and the Kuroshio under the LM path, although research on the effects of the Kuroshio path on synoptic-scale atmospheric conditions and climate over Japan is ongoing.

3.2. Influence of the KE on the atmosphere

3.2.1. Climatological features

The KE path is characterized by two quasi-stationary meanders with ridges located around 144°E and 149°E (Fig. R22-5). The strong SST front, which reflects subsurface oceanic conditions with a strong temperature front (Nonaka et al., 2006), occurs at about 36°N along the KE northern boundary.

Along this SST front, the THF also exhibits a strong frontal gradient, and both a SST front and a cross-frontal contrast in heat flux are observed in winter (Fig. R22-6a). The horizontal SST gradient exceeds 5°C (100 km^{-1}) in winter, and the corresponding gradient in THF reaches 100 W m^{-2} (100 km^{-1}). Owing to a sharp cross-frontal contrast in heat release to the atmosphere, this oceanic frontal zone may play a crucial role in intensifying atmospheric baroclinicity and thereby maintaining the North Pacific storm track (Nakamura et al., 2004a, b). The wintertime large upward THF along the KE warms the overlying marine atmospheric boundary layer (MABL) locally, forming a sea level pressure trough (Tanimoto et al., 2011) and an associated local maximum of cloudiness (Tokinaga et al., 2009). Extratropical cyclones develop explosively over the KE in winter (Gyakum et al., 1989; Chen et al., 2002). These can be similar in strength to tropical cyclones and can lead to severe weather disasters caused by heavy rainfall/snowfall, strong winds, and high waves on the Pacific side of the Japanese islands. The explosive development of extratropical cyclones is induced by baroclinic instability in association with the SST front along the KE (Yoshiike and Kawamura 2009; Iizuka et al., 2013) and diabatic heating processes through precipitation over the warm KE (e.g., Yoshida and Asuma 2004; Kuwano-Yoshida and Asuma 2008; Kuwano-Yoshida and Minobe 2017; Iwao et al., 2012; Hirata et al., 2015).

In summer, the SST gradient and THF gradient drop to about 2°C (100 km^{-1}) and 20 W m^{-2} (100 km^{-1}), respectively (Fig. R22-6b). However, the KE has a distinct impact on the overlying atmosphere; fog formation is likely over the cold water north of the KE under the warm, moist southerly winds (Tanimoto et al., 2009; Tokinaga et al., 2009), whereas the formation of convective stratocumulus is most likely over the warm KE under cold northerly winds (Tanimoto et al., 2009; Tomita et al., 2013; Kawai et al., 2015). Pressures in the MABL on the warm side of the SST front along the KE northern boundary become higher than those on its north side, and its associated northward pressure gradient forms easterly winds (Nishikawa et al., 2016). The SST front along the KE northern boundary induces a narrow band of surface wind convergence due to a pressure adjustment process, influencing the baiu rainband (Tokinaga et al., 2009).

3.2.2. Decadal-scale variability of the KE path

3.2.2.1. Meridional movement

The KE path shows a meridional movement with an amplitude of about 200 km in latitude (Qiu and Chen 2005, 2010; Nonaka et al., 2006; Joyce et al., 2009) on a decadal time scale (Seo et al., 2014). The meridional movement of the KE path is initiated by wind-induced Rossby waves formed in the central North Pacific (Miller et al., 1998; Deser et al., 1999; Seager et al., 2001; Schneider et al., 2002; Qiu 2003; Taguchi et al., 2005, 2007; Qiu and Chen 2005, 2010; Qiu at al. 2014; Nonaka et al., 2006; Ceballos et al., 2009), the major driving forcing of which is the decadal-scale meridional movement of the Aleutian Low (AL) located in central North Pacific (Sugimoto and Hanawa 2009; Seo et al., 2014). Negative wind stress curl anomalies around 35°N in the central/eastern North Pacific associated with a northward shift of the AL induce a deepening of the main thermocline, and this deepening signal then propagates westward, reaching the KE region after about 3 years, where it causes the KE path to move northward.

The meridional movement of the KE path yields strong SST anomalies between 34°N and 36°N, leading to significant changes in the near-surface synoptic-scale atmospheric field in winter (Joyce et al., 2009) and inducing meridional movement of the baiu rainband in summer (Matsumura et al., 2016).

3.2.2.2. Path perturbations

The KE path has two dominant states (Qiu and Chen 2005, 2010), an unstable state when the meanders become more obscure in 1995–2001 and 2006–2009, and a stable state with two quasi-stationary meanders in 1993–1994, 2002–2005, and 2010–2016 (Figure R22-5). The path states of the KE (stable/unstable path) modulate on a decadal

timescale (Qiu and Chen 2005, 2010), but the period is somewhat shorter than that of the meridional movement of the KE path. In fact, there is no significant correlation between the two (Seo et al., 2014). The KE path state is related to the path of the Kuroshio south of Japan (Sugimoto and Hanawa 2012; Usui et al., 2013; Seo et al., 2014). The KE path adopts a relatively stable state when the Kuroshio goes through a deeper channel of the Izu Ridge (about 2500 m water depth), but tends to be convoluted (unstable) when the Kuroshio passes over shallower parts of the Izu Ridge (about 1000 m water depth).

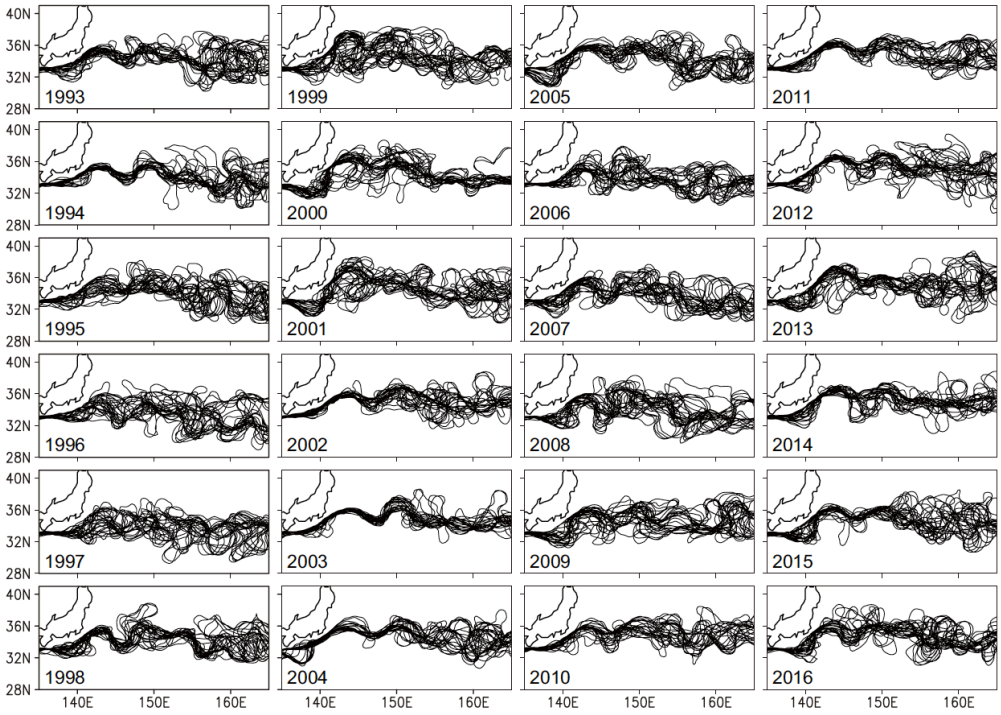

Figure R22-5. Yearly paths of the Kuroshio and KE plotted every 14 days using satellite-derived sea surface height (SSH) data from the Copernicus Marine Environment Monitoring Service (CMEMS).

The path state exerts a strong influence on oceanic/atmospheric conditions on both the north and south sides of the KE path. On the south side of the KE, an unstable (stable) path strengthens (weakens) subsurface ocean stratification through strong (weak) eddy activity (Qiu and Chen 2006; Qiu et al., 2007; Sugimoto and Kako. 2016), resulting in a shallower (deeper) winter ocean mixed layer (Qiu et al., 2007; Oka et al., 2012; Sugimoto and Kako 2016). The shallower (deeper) periods of the winter ocean mixed layer induce weak (strong) vertical entrainment, forming a positive (negative) anomaly of temperature tendency. This results in the decadal-scale surface ocean temperature variations in winter. The surface ocean temperature, in turn, determines the magnitude of the upward THF release (Sugimoto and Kako 2016). On the north side of the KE

(i.e., the Kuroshio–Oyashio Confluence region) in the unstable state, anticyclonic mesoscale ocean eddies, with a horizontal extent of a few hundred kilometers and a thickness of a few hundred meters, pinch off from the KE in a northward direction (Itoh and Yasuda 2010; Sugimoto and Hanawa 2011; Sasaki and Minobe 2015), resulting in warm, salty conditions (Sugimoto and Hanawa 2011; Kouketsu et al., 2012; Seo et al., 2014) and a deepening of the winter ocean mixed layer (Kouketsu et al., 2012; Oka et al., 2012; Kawakami et al., 2016). The positive SST anomalies attributable to anticyclonic (warm) eddies are primarily responsible for the upward THF release (Sugimoto and Hanawa 2011; Sugimoto 2014) and the acceleration of surface winds due to the vertical mixing effect (Sugimoto et al., 2017) (Fig. R22-6). The enhanced THF from the warm eddies heats the MABL locally and thereby increases local cloudiness and precipitation (Masunaga et al., 2015, 2016; Sugimoto et al., 2017).

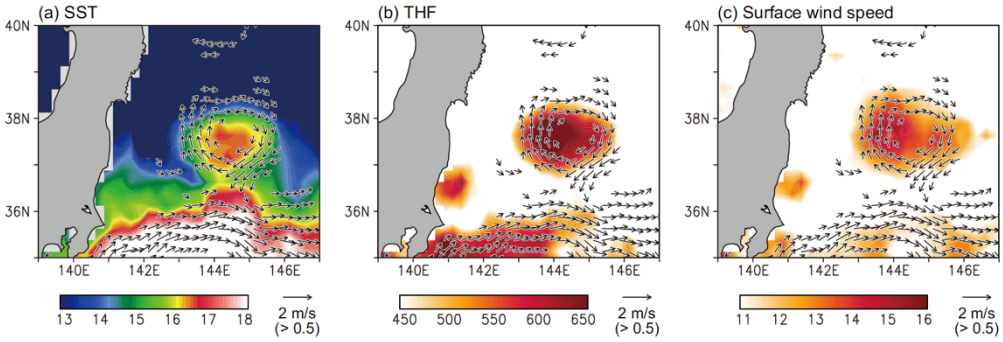

Figure R22-6. Snap shots for 30 January 2002 of (a) SST (°C), (b) upward thermal heat flux (THF, W m^{-2}), and (c) surface wind speed (m s^{-1}) from the J-OFURO3. Arrows represent sea surface velocity vectors from the CMEMS, and small velocity vectors (< 0.5 m s^{-1}) are removed.

4. Oceanography

4.1. Hydrography The long-term Kuroshio variation off the southern coast of Honshu

(Yugo Shimizu, Keiichi Yamazaki, Takeshi Okunishi, Takashi Setou and Kiyotaka Hidaka)

The Kuroshio is a western boundary current in the North Pacific subtropical gyre, and flows northeastward with speed about 1–3 m s^{-1} at the surface off the southern coast of the Japanese islands. As to the long-term temperature change of the Kuroshio water, Wu et al., (2012) showed that the sea surface ocean warming was enhanced in the western boundary current areas in the subtropical gyres and the warming rate of the Kuroshio area was 1.1–1.3 °C per century from 1900–2008 whereas the global mean

was 0.6–0.7 °C per century. As for salinity change, Ren and Riser (2010) showed that salinity has been decreasing in the subtropical thermocline of the North Pacific Ocean since the 1980s. If the Kuroshio sea surface water has been warming and freshening in these few recent decades, the baroclinic structure and thus the current speed can change. As a result, the poleward heat flux by the Kuroshio can change to cause climate change. Using an air–sea coupling model simulation with an annual CO_2 increase of 1 % scenario, Sakamoto et al., (2005) showed that the speed of the Kuroshio and its extension increases up to the maximum 0.3 m s^{-1} after a century. The change in speed of the Kuroshio current is thought to have an influence on the reproduction, recruitment and resource of the fishes spawning in the Kuroshio area. For example, the inshore region north of the Kuroshio front is an important spawning and nursery ground for pelagic fishes such as Japanese sardine and mackerel. The juveniles of these fishes utilize the Kuroshio to migrate to the Kuroshio–Oyashio transition area, which is their feeding ground, so the Kuroshio change in speed influences their migration period.

Since the studies above have been based on a database or simulation in gyre-century scale, the description on time changes of Kuroshio water properties based on hydrographic observation at a smaller time–spatial scale is needed to further understand longer-term variability. In this subsection, we describe the time change characteristics in observed salinity, temperature and density based on the repeat hydrographic observation section along 138˚E (the O-line; Figure R22-7) during January 2000 to March 2018, which was carried out mainly using a Conductivity-Temperature-Depth sensor (CTD; 911 plus, Seabird Co., USA) in January, March, May, August and October ± one month by the R/V *Soyo-Maru* of the Fisheries Research Institute of Fisheries Science (Yokohama), Japan Fisheries Research and Education Agency.

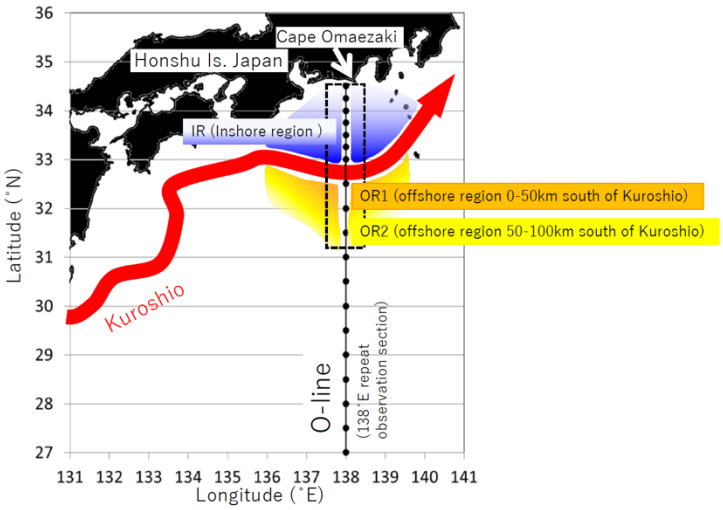

Figure R22-7. Location of the 138°E repeat hydrographic observation section off Cape Omaezaki (O-line) and schematic representation of the Kuroshio path (red thick arrow). The regions defined for the present SST analysis (Figure R22-6) are indicated by blue, orange, and yellow areas enclosed by a broken line.

As the Kuroshio path changes temporally (Kawabe 1985), we analyzed these time changes with a locational reference to the Kuroshio axis. The latitude of the Kuroshio axis on 138°E was defined as a position of the 1000 dbar-referenced geostrophic current maximum at 10 m depth. An example of a vertical section along this section shows that the Kuroshio axis (the current maximum location at the sea surface) was located at 33°40'N in geostrophic current section while the indicative isotherm at 200 m depth (T_{200m} = 15°C), which was suggested by Kawai (1969), was seen at about 33°45'N with steep frontal structure of salinity and density (Figure R22-8). We will later discuss the agreement/disagreement in the positions between the indicative isotherm of Kawai (1969) and the surface current speed maximum of the Kuroshio axis.

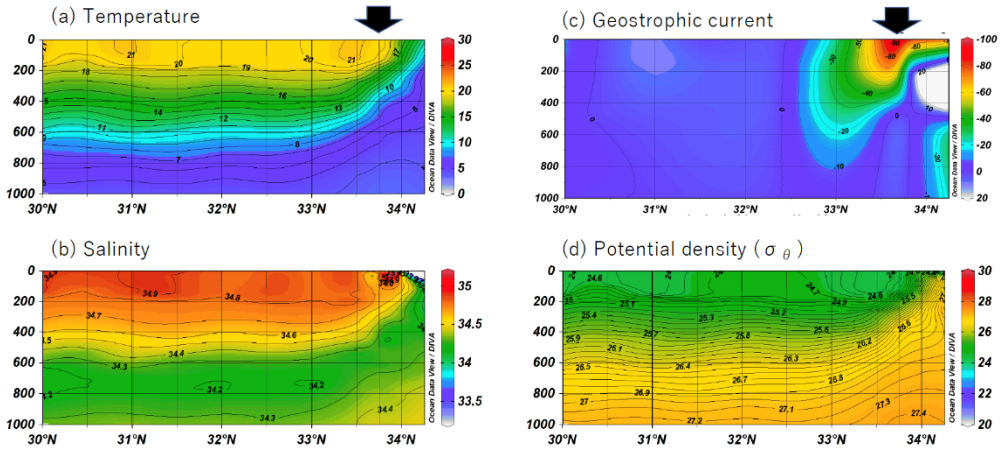

Figure R22-8. Vertical sections (latitude – pressure [dbar]) along the 138°E repeat

hydrographic observation section off Cape Omaezaki (O-line). (a) Temperature (°C), (b) salinity, (c) geostrophic current (positive eastward) referenced to 1000 dbar (cm s^{-1}) and (d) potential density (σ_θ) in March 2003 by the R/V *Soyo-Maru*, Fisheries Research Institute of Fisheries Science (Yokohama), Japan Fisheries and Education Agency. The location of the Kuroshio axis according to the indicative isotherm of (Kawai 1969) and geostrophic current maximum at the sea surface are indicated by thick black arrows in (a) and (c), respectively.

The time series of the observed temperature, salinity and density on the Kuroshio axis on the O-line (Figure R22-9) shows a clear seasonal variability, especially in the upper layers. The mean temperature, salinity and density on the Kuroshio axis averaged in each observation month changes more clearly at the shallower depths (Figure R22-10). The mean temperature reaches the minimum in March at 10–150 m depth and in May at 200 m depth, whereas it reaches the maximum in August at 10–50 m depths, and in October at 75–200 m depths (Figure R22-10a). The monthly change in the mean salinity is similar to the temperature if the word “maximum” in the temperature change is replaced by “minimum” in salinity change, except for the salinity minima in May at 150 and 200 m depths (Figure R22-10b). As a result, the mean density takes the minimum in August at 10 and 50 m depths, and in October at the deeper depths. Thus, there is a clear seasonal change, especially at shallower depths, and followed by time lags when the minimum (maximum) propagates from upper to deeper layers in temperature and salinity below the Kuroshio axis.

Since the analyzed O-line observation period 17 years was too short to detect decadal- or century-scale time change, another analysis is needed to assume the change is longer than the seasonal. Sea surface temperature (SST) data have been collected from satellites, and NOAA publishes objectively interpolated SST (OISST) since 1982. We also have the Kuroshio path position published by the Japan Coast Guard, which can be purchased from MIRC (http://www.mirc.jha.or.jp/products/KCP/). The SST change in the areas around the Kuroshio axis was examined along 138°E (Figure R22-11). As a result, the annual mean OISST in each area around the Kuroshio showed a significant increase trends (Figure R22-11), and the most intense warming is seen in the Kuroshio current area (±25 km north/south of the Kuroshio axis,). Also, there seems to be a tendency that the SST in each area increases up to 1998 and then decreases after 1999, and thus the analysis period on the O-line data seems to correspond to a cooling period in decadal scale.

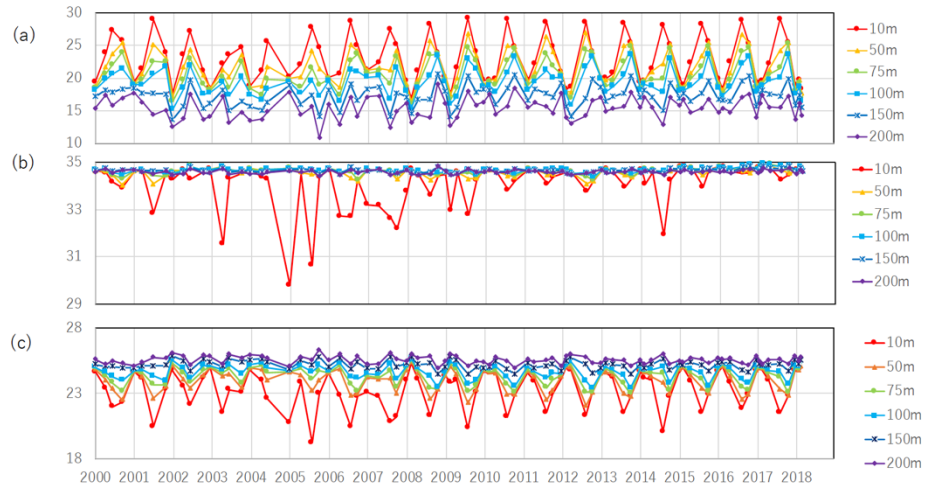

Figure R22-9. Time series of (a) temperature (°C), (b) salinity and (c) potential density (σ_θ) at the Kuroshio axis (defined as the geostrophic current maximum at 10 m depth) observed on the 138°E repeat observation section (O-line) during January 2000–March 2018.

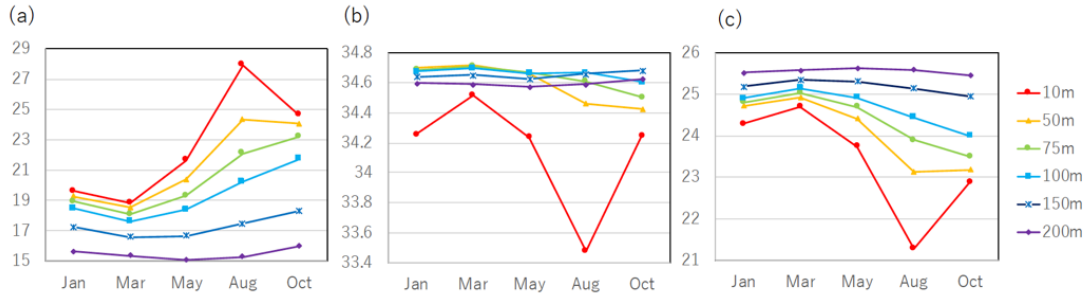

Figure R22-10. (a) Mean temperature (°C), (b) salinity and (c) potential density (σ_θ) at the Kuroshio axis (defined as the geostrophic current maximum at 10 m depth) in each observation month on the 138°E repeat observation section (O-line) during 2000–2017.

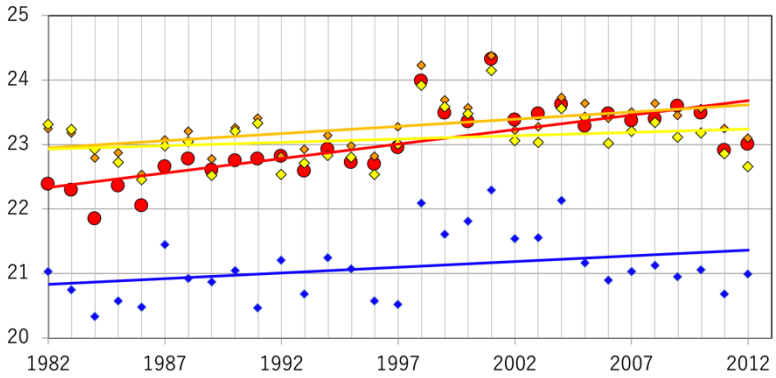

Figure R22-11. Time series of annual mean sea surface temperature (SST; [°C) from NOAA daily OISST (https://www.ncei.noaa.gov/products/optimum-interpolation-sst) in each area indicated in Figure R22-2 (red, Kuroshio current: blue, inshore region: orange, offshore region 1 and yellow, offshore region 2 with a latitudinal reference to the Kuroshio path published by Japan Coast Guard) at 138°E ± 0.5°E during year 1982–2012 with linear fitted lines.

It was over 50 years ago that Kawai (1969) showed the indicative isotherm of the Kuroshio axis off the southern coast of Japan. Comparison between the indicative isotherm of Kawai (1969) and the one estimated from present data might be effective to assume the long-term change at 200 m depth below the Kuroshio. Kawai (1969) estimated the isotherm by fitting the observed temperature at 200 m depth at the sea surface current maximum observed by the GEK (geomagnetic electro-kinetograph) around the Kuroshio strong current using 1960s data. We estimated the indicative isotherm below the 1000 dbar-referenced geostrophic current maximum at 10 m depth (Table R22-1, 200 m depth temperature values in Figure R22-9a), whose annual mean is 0.5°C higher than Kawai's (1969) indicative isotherm. Does it mean that temperature at 200 m depth below the surface Kuroshio current maximum has warmed after these 50 years? Kawai (1969) suggested the Kuroshio indicative isotherms by 0.5°C intervals off the landmark capes of the southern coast of Japan. On the other hand, there seems to be a seasonal change in temperature at 200 m depth, and the standard deviation is not negligible for the present estimate (Table R22-1). Furthermore, our estimating method is slightly different from Kawai's (1969) since we estimate it by using geostrophic current maximum. Thus, we cannot precisely evaluate the 0.5°C difference between his indicative isotherm and our present estimate for the time being.

Table R22-1. Mean temperature at 200 m depth below the 1000-dbar referenced geostrophic current maximum at 10 m depth around the Kuroshio, standard deviation (S.D.) and averaged data number (N) in each observational month on 138°E repeat observation section (O-line) during 2000–2017.

Obs. month	T_{200m} [°C]	S.D.[°C]	N
January	15.6	1.6	18
March	15.3	1.7	11
May	15.1	1.4	18
August	15.3	1.6	18
October	16.0	2.0	17
Mean/Total	15.5	1.7	82

Since clear seasonal variability in temperature and salinity is found in the present study, further study should reveal the longer-term change in each season, focusing on the seasonal change mechanism. For this, we must continue monitoring the Kuroshio to detect the decadal-to-century scale time change more accurately with seasonal observations.

4.2. Nutrients variation in Kuroshio Area

(Tsuneo Ono)

Vertical distribution of nutrients in the Kuroshio area has been monitored along 137°E by the Japan Meteorological Agency (JMA) twice a year from 1967 to the present (http://www.data.jma.go.jp/gmd/kaiyou/db/vessel_obs/data-report/html/ship/ship_e.php). In 2002, the Japan Fisheries Research and Education Agency (FRA) started an additional repeat hydrographic observation line from 30°N to 34.75°N along 138°E called the “O-line” (Sugisaki 2010) with an observation frequency of five times a year. Kodama et al., (2014) summarized nutrient data observed along the O-line from 2002 to 2013 and analyzed their inter-annual variability. He divided the data into three oceanographic areas: the Kuroshio core (defined by the nearest quick bulletin of ocean conditions by the Japan Coast Guard, https://www1.kaiho.mlit.go.jp/jhd-E.html), south of Kuroshio core (hereafter “gyre” area), and the water between the Japan coast and Kuroshio core (hereafter “slope” area). Temporal variation of area-averaged nutrient content was then analyzed. Both the Kuroshio core and gyre area showed little inter-annual variation in the upper 200 m of the water column, while the slope area showed significant inter-annual variation in the depth of the nutricline, with a deepening trend after 2010 (Figure R22-12).

Surface concentration of nitrate + nitrite in the winter slope area also showed inter-annual variation, and it was negatively correlated to the difference in depth between the bottom of mixed layer (Z_m) and the nutricline (i.e., depth where the concentration of nitrate + nitrite becomes 15 m, Z_{15}). The variability of Z_{15} was far larger than that of Z_m, where the surface concentration of winter nitrate is mainly controlled by the variability of Z_{15}.

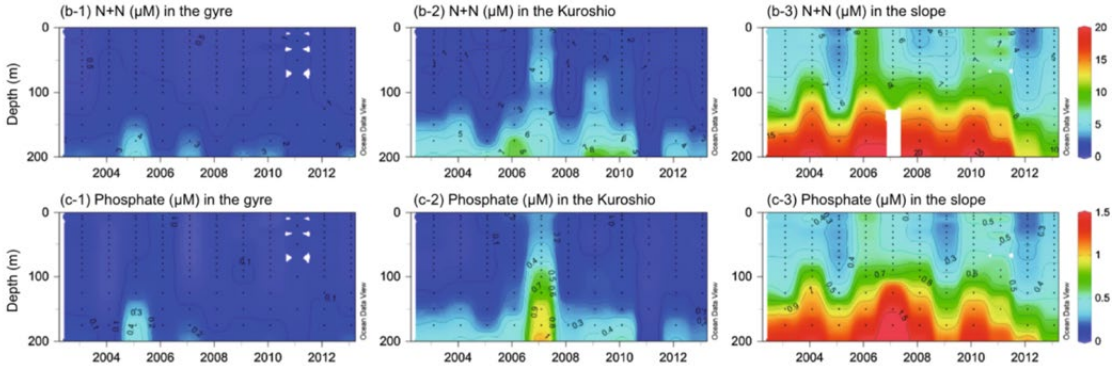

Figure R22-12. Temporal variation of the vertical distribution of nitrate + nitrite (upper panel) and phosphate (lower panel), respectively, averaged for each area along 138°E. After (Kodama et al., 2014).

Unfortunately, we have no nutrient data along 138°E before 2002. A more recent study, however, showed that Z_{15} can be estimated as an isopycnal depth of σ_θ = 25.96 (Ono et al., 2015). We, therefore, are able to estimate the temporal variation of Z_{15} from historical CTD data only, and the temporal variation of winter surface nutrient content can also be estimated qualitatively by using the observed relationship between Z_{15} and winter surface nutrient concentration. Figure R22-13 shows estimated Z_{15} time series from 1970 to present, using data from regular CTD observation lines of the Shizuoka Prefectural Fisheries Experiment Station. The obtained time series shows a long-term shoaling trend of –1.5 ± 0.4 m/y. This indicates that the surface concentration of nitrate in the winter slope area had increased, although recent deepening of Z_{15} (Figure R22-12) might be the cause of tentative nitrate reduction in the winter mixed layer of the slope area.

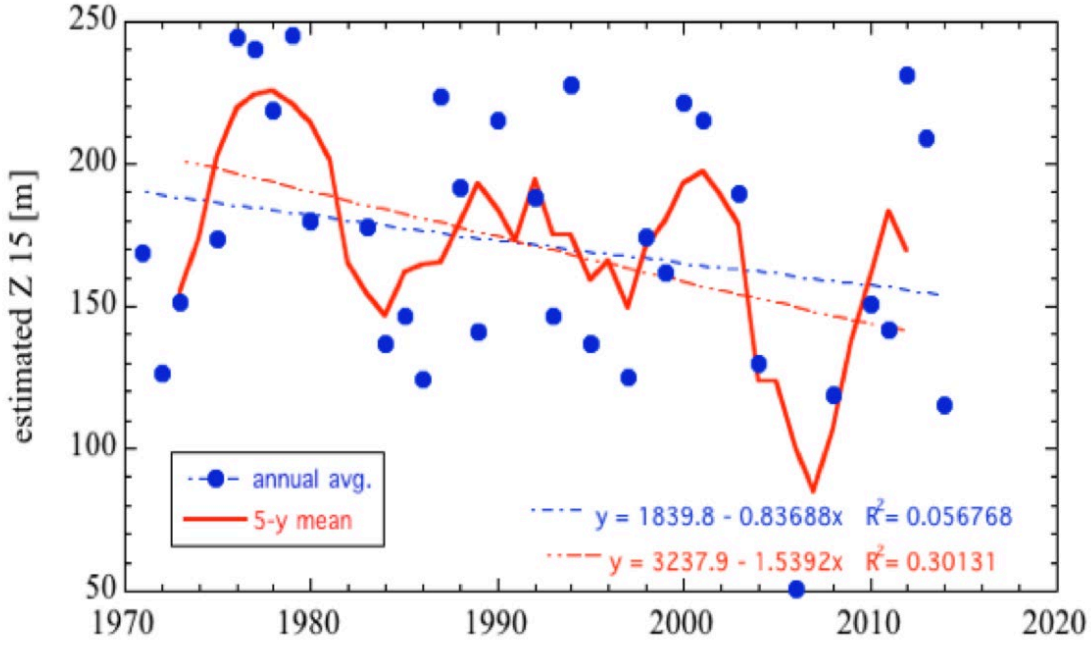

Figure R22-13. Temporal variation of Z_{15} estimated as depth of isopycnals σ_θ = 25.96. Historical CTD data observed by Shizuoka Prefectural Fisheries Experiment Station were used for calculation of σ_θ.

5. Phytoplankton

(Kiyotaka Hidaka)

Primary producers in the Kuroshio and its adjacent areas south of Honshu support important spawning grounds for pelagic fishes such as sardine, anchovy and Pacific saury. Seasonal change in satellite chlorophyll have been reported in several articles (e.g., Hidaka and Nakata 2010; Kodama et al., 2014; Sugisaki 2010). In this section, seasonal change of sea surface chlorophyll concentration, along with sea surface temperature, were compiled for the area south of Japan, including area west of Cape Shionomisaki, which have not been reported since the previous North Pacific Ecosystem Status Report (NPESR).The area was divided into west (131°00'E–136°00'E) and east (136°00'E–139°00'E) sections at about Cape Shionomisaki and data compiled for the slope water and the Kuroshio in each section. Slope water is defined as the area between the 1000 m isobaths on the continental slope and 56 km north of the Kuroshio axis (Figure R22-14). The data manipulations were similar to those in the previous NPESR, but calculated based on the ESA Ocean Color CCI (http,//www.esa-oceancolour-cci.org) while the calculation in the previous NPESR was based on SeaWiFS (https://oceancolor.gsfc.nasa.gov/data/seawifs/).

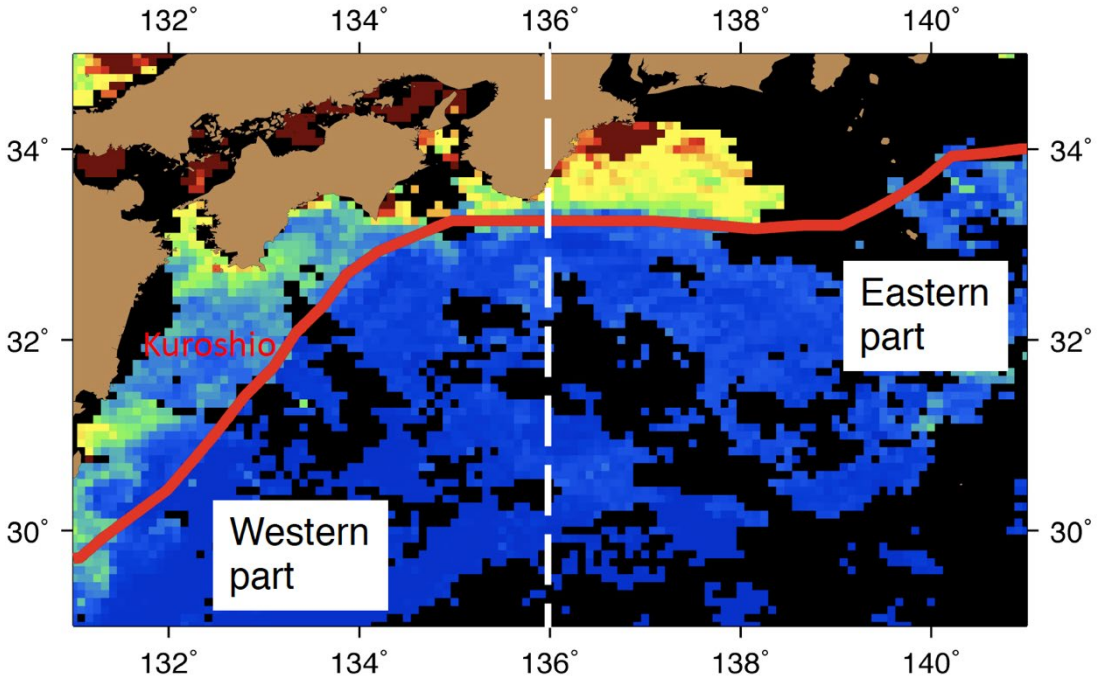

Figure R22-14. The area analyzed for satellite chlorophyll in the Kuroshio region.

Figure R22-15 shows seasonal change of sea surface temperature (SST) and surface chlorophyll a concentration. Slope water had higher chlorophyll a concentration than the Kuroshio (Figure R22-15a). The seasonal cycle of chlorophyll a in the Kuroshio was similar in the east and the west with a peak in the late March (Figure R22-15b). The pattern in the slope water in the western part was similar although chlorophyll a was higher than in the Kuroshio. The eastern part of the slope water showed a different seasonal pattern. Chlorophyll a concentration there started to increase from the end of February (day 56–64) and reached maximum values (0.74–0.80 μg l^{-1}) in March (day 88–96) as in the western part. But the sequence after mid-March differed and high chlorophyll a (>0.6 μg l^{-1}) remained until mid-May (ca. day 144).

Seasonal variation of chlorophyll a is well synchronized with SST in both regions. Blooms start at the end of the low temperature season (<16.3˚C, day 32–72) and decrease as SST increases (day 120–240). The trends described above were consistent among those reported in the previous NPESR and the current analysis in each area.

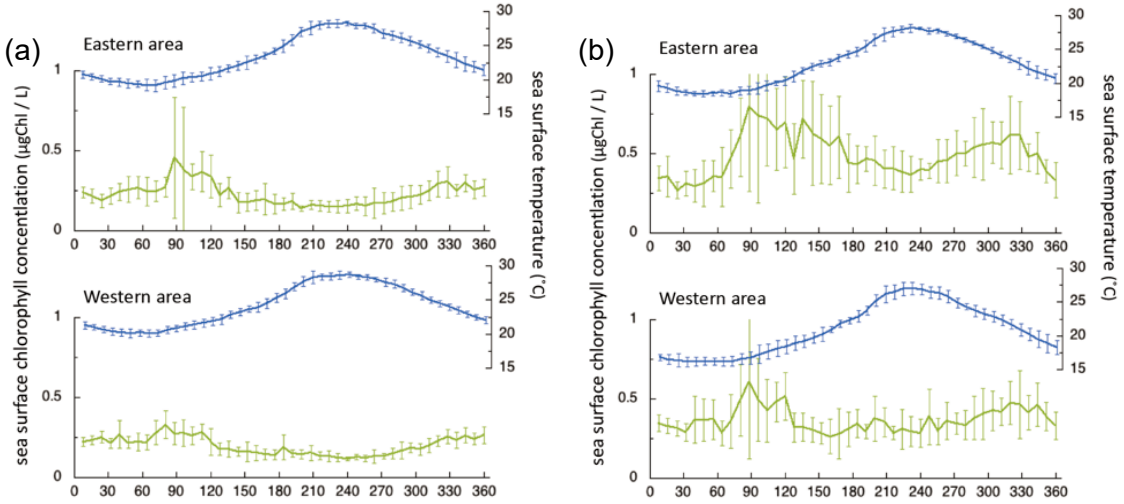

Figure R22-15. (a) Seasonal change of sea surface temperature and sea surface chlorophyll-a concentration in the slope water. (b) Seasonal change of sea surface temperature and sea surface chlorophyll-a concentration in the Kuroshio area.

6. Zooplankton

(Kiyotaka Hidaka)

Zooplankton in the area is mainly composed of copepods, chaetognaths, and appendicularians (Kidachi and Ito 1979; Nakata and Hidaka 2003). In this section, the zooplankton population in winter-to-spring is focused as it is when major forage fishes prey on them in the area. Kidachi and Ito (1979) described zooplankton composition and horizontal distribution during the spring season. Recently, Miyamoto et al., (2017) have conducted a more sophisticated analysis on the data collected in a monitoring line located in the eastern region off Honshu. Their analysis identified five copepod assemblages distributed meridionally relative to the Kuroshio axis. The abundance of copepods was highest in the north-frontal area of the Kuroshio and abundance of copepod species in each assemblage was affected by the position of the Kuroshio axis. In the analysis of copepod communities, *Calanus sinicus* and *Paracalanus parvus* s.l. have been regarded as important species in the area by their abundance (Sogawa et al., 2017, 2019). The latter has also been regarded as major prey items for larvae and juveniles of forage fish (e.g., Takagi et al., 2009; Okazaki et al., 2019). Recently, *C. sinicus* has also been found to be important in this context, as it has been suggested that larvae of Japanese sardine and Pacific round herring prey mainly on the nauplii of C. *sinicus* (Hirai et al., 2017) in the Tasa Bay.

Nakata and Hidaka (2003) and Nakata and Koyama (2003) have described the long-term fluctuation of the zooplankton in the area.

The annual variation of copepod biomass in the following period of those reports was obtained by means of a bench-top model of the Video Plankton Recorder (Ichikawa et al., 2009). Figure R22-16 shows the annual variation of copepod biomass in February to March in the slope water south of Honshu in the period following that described in Nakata and Hidaka (2003). The eastern area shows that the biomass was relatively stable in 2004–2010 and a large increase in biomass was observed after 2010 and 2012, and remains sustained. In the western area, a large copepod biomass was seen in 2003, 2007, 2008 and 2013. It should be noted that copepod biomass in the western area in each year was comparable to that in the eastern area, with higher biomass in 6 of 17 years. The trend is different from that seen in sea surface chlorophyll concentration, which was higher throughout the year in the eastern area. The higher biomass in the western area could have been brought about by higher water temperature that could enhance production of zooplankton, or be reflected in the production in the upstream region of the Kuroshio.

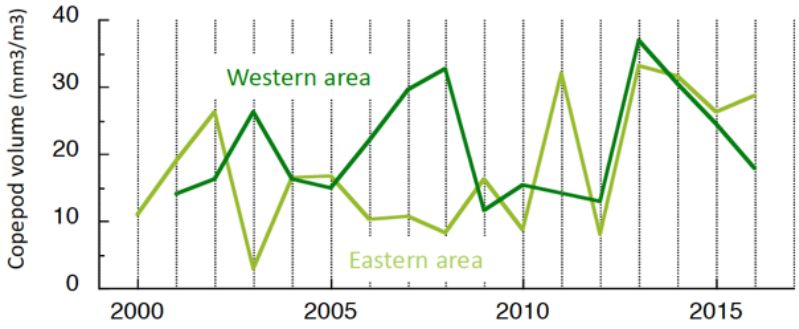

Figure R22-16. Annual variation of copepod biomass in February to March in the slope water south of Honshu, Japan.

7. Pelagic fishes

(Akinori Takasuka, Yoshioki Oozeki)

7.1. Pelagic fish community

Small pelagic fish are widely distributed, migrate, and spawn in the Kuroshio Current system off the Pacific coast of Japan. The pelagic fish community in this system includes Japanese sardine (*Sardinops melanostictus*), Japanese anchovy (*Engraulis japonicus*), round herring (*Etrumeus micropus*), chub mackerel (*Scomber japonicus*), spotted mackerel (*Scomber australasicus*), Japanese jack mackerel (*Trachurus japonicus*), Pacific saury (*Cololabis saira*), and Japanese common squid (*Todarodes pacificus*), although their distributions do not necessarily overlap seasonally and

spatially. Typically, sardine, anchovy, mackerel, saury, and common squid spawn in the coastal areas off the Pacific coast of Japan with some differences in main spawning seasons. Their eggs and larvae are transported offshore by the Kuroshio Current. Then, the juveniles migrate northward from the Kuroshio Extension to the Kuroshio–Oyashio transition regions. Thus, the Kuroshio Current system mainly provides their spawning and nursery grounds. There, large pelagic fish such as skipjack tuna (*Katsuwonus pelamis*), blue shark (*Prionace glauca*), and neon flying squid (*Ommastrephes bartramii*) are predators for these small pelagic fish. Jack mackerel spawn mainly in the East China Sea and are transported by the Kuroshio to the Pacific coastal areas off Japan. Round herring spawn and inhabit these coastal areas as well.

7.1.1. Population dynamics

Small pelagic fish exhibit cyclic and dramatic population dynamics in response to climate variability at multidecadal scales. A typical example is the out-of-phase population oscillations between sardine (*Sardinops* spp.) and anchovy (*Engraulis* spp.) in the Kuroshio, California, Humboldt, and Benguela Current systems (Kawasaki 1983; Lluch-Belda et al., 1989; Chavez et al., 2003). In the Kuroshio Current system, sardine populations were very abundant during the 1980s, while anchovy populations were relatively scarce during the same period (Fig. 17a,b).

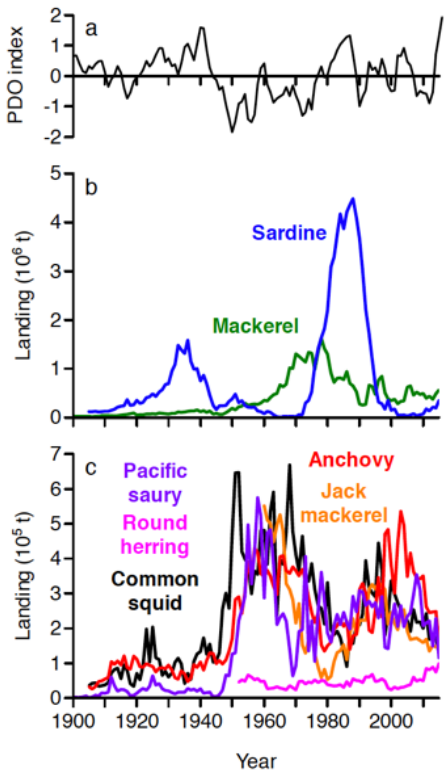

Figure R22-17. Long-term landing histories of small pelagic fish in waters around Japan in relation to climate variability. (a) Pacific Decadal Oscillation (PDO) index,

which is defined as the leading principal component of monthly sea surface temperature (SST) anomalies in the North Pacific, poleward of 20°N (monthly mean global average SST anomalies were removed) (Mantua and Hare 2002). (b) Japanese sardine (*Sardinops melanostictus*) and mackerel (*Scomber* spp.). (c) Japanese anchovy (*Engraulis japonicus*), Japanese jack mackerel (*Trachurus japonicus*), Pacific saury (*Cololabis saira*), round herring (*Etrumeus* teres), and Japanese common squid (*Todarodes pacificus*). The landing data were updated from Yatsu and Kaeriyama (2005) and Takasuka et al., (2008b) and were originally based on the data set from Statistics of Agriculture, Forestry and Fisheries.

However, sardine populations then decreased markedly at the end of the 1980s and subsequently have experienced very low levels during the last few decades. In contrast, anchovy populations have increased in abundance during the period of low sardine biomass. The patterns of such “species alternations” have been closely related to multidecadal climate variability (Takasuka et al., 2007, 2008b), as being represented by the Pacific Decadal Oscillation (PDO) index (Mantua and Hare 2002). When the PDO index is positive, the sea surface tends to be cooler in the western North Pacific. During this period, sardine populations flourish in the Kuroshio Current system. In contrast, when the PDO index is negative, the sea surface tends to be warmer, and anchovy populations flourish in the Kuroshio Current system. The relationship of the species alternations to the temperature regimes in the Kuroshio Current system shows a marked contrast to the case in the eastern Pacific, where the sardine populations tend to be abundant during the warm regimes related to positive anomalies of the PDO index and the anchovy populations tend to be abundant during the cool regimes related to negative anomalies of the PDO index (Mantua and Hare 2002; Chavez et al., 2003; Takasuka et al., 2008c).

Similar population dynamics in response to the PDO index have also been observed in multidecadal trends in landing histories of mackerel (chub mackerel and spotted mackerel), jack mackerel, and common squid (Figure R22-17). Mackerel populations were abundant during the late 1970s, between the high-biomass periods of anchovy (the 1960s) and sardine (the late 1980s). In contrast, jack mackerel and common squid have shown very similar population dynamics to anchovy. However, round herring have shown relatively stable patterns of population dynamics. Of note is the marked difference in the extent of population fluctuations among these species (Takasuka et al., 2008b). For example, the maximum biomass is more than 10 times greater for sardine than for anchovy in the stock assessment data (FRA 2017). The extent of population fluctuation is approximately 20 times greater for sardine than for anchovy.

Of great interest is the current status of the pelagic fish community in the Kuroshio Current system. Since the late 1980s, sardine have experienced very low population

levels , whereas anchovy, jack mackerel, and common squid have experienced relatively high levels of population. Recently, however, sardine populations have started to increase, showing a sign of their population recovery. In contrast, the population levels of anchovy, jack mackerel, and common squid are now declining simultaneously. As such, the pelagic fish community in the Kuroshio Current system may be experiencing a shift to a new regime.

7.1.2. Distribution and spawning ground

The distribution areas and spawning grounds of small pelagic fish change with their population dynamics. The spawning grounds expand to offshore waters during the high-biomass periods and contract to inshore waters during the low-biomass periods in sardine and anchovy in the Kuroshio Current system (Watanabe et al., 1996; Oozeki et al., 2007; Takasuka et al., 2008a). Such expansion and contraction of distribution areas are general phenomena in small pelagic fish. Barange et al., (2009) examined the stock biomass and distribution area of sardine and anchovy in the Kuroshio, California, Humboldt, and Benguela Current systems to find allometric relationships between distribution area and stock biomass. In this subsection, some examples of spatial dynamics are shown for spawning grounds of sardine and anchovy and larval distributions of saury, based on the data of egg and larval surveys in the Kuroshio Current system.

Egg surveys have been conducted extensively off the Pacific coast of Japan on a monthly basis since 1978 (Oozeki et al., 2007; Takasuka et al., 2008a). The surveys are intended to monitor egg abundance and distribution of major small pelagic fish throughout the year. In the surveys, plankton nets with mouth ring diameters of 45 or 60 cm and mesh sizes of 0.330 or 0.335 mm are towed vertically from 150 m depth. Monthly egg abundance is calculated by a combination of the mean egg density, survival rate, and egg incubation time at a 15’ × 15’ square level for major small pelagic fish.

Monthly egg abundance distributions for sardine in February are shown in Figure R22-18. The spawning season of sardine is limited from late-winter to early-spring seasons with a peak in February to March. In February, they spawn mainly in the western areas off the Pacific coast of Japan, then start to spawn in the eastern areas in later months. In 1988 (high-biomass period), sardine spawned intensively and widely in the western areas, and their spawning grounds were also observed in the offshore waters. In 2004 and 2010 (low-biomass period), however, they spawned only in the inshore waters, and their spawning grounds were limited to several bay and channel areas. In recent years (e.g. 2015), sardine have spawned more intensively and widely than in the last decade. In addition, they have also spawned in the eastern areas even in February.

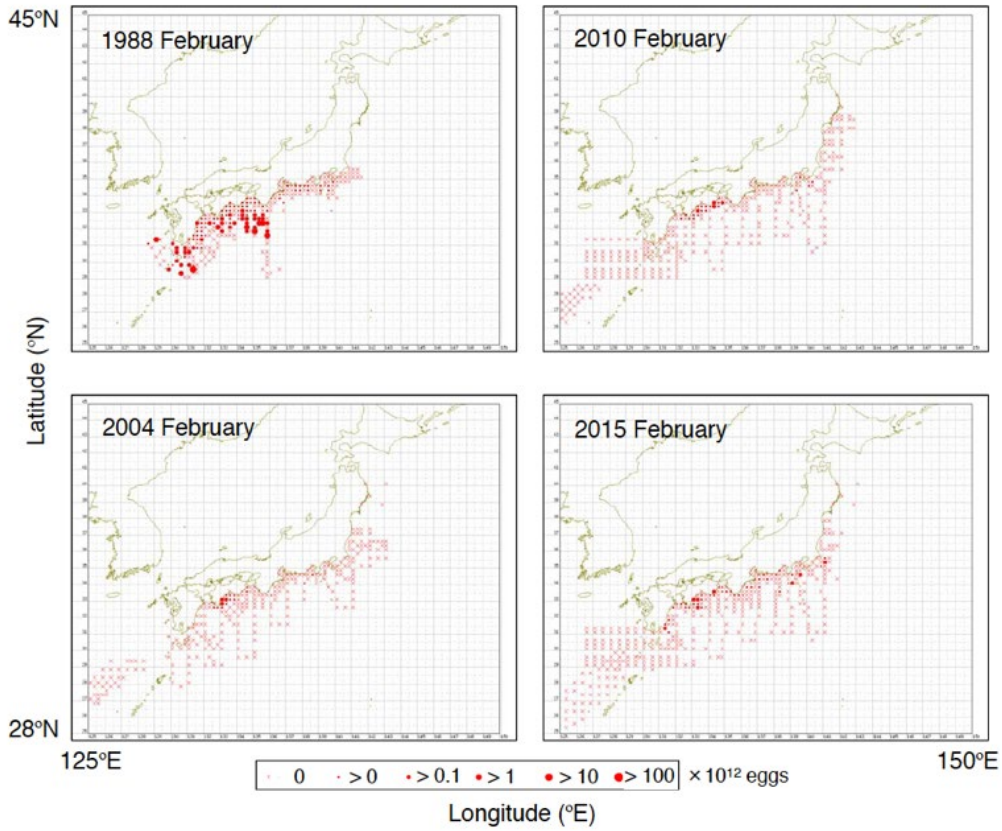

Figure R22-18. Monthly egg abundance distribution of Japanese sardine (*Sardinops melanostictus*) in February (main spawning month for sardine) in 1988 (high-biomass period), 2004 (low-biomass period), 2010 (low-biomass period), and 2015 (recent year). Monthly egg abundance was calculated by a combination of the mean egg density, survival rate, and egg incubation time at a 15' × 15' square level, based on an egg survey data set (Takasuka et al., 2008a).

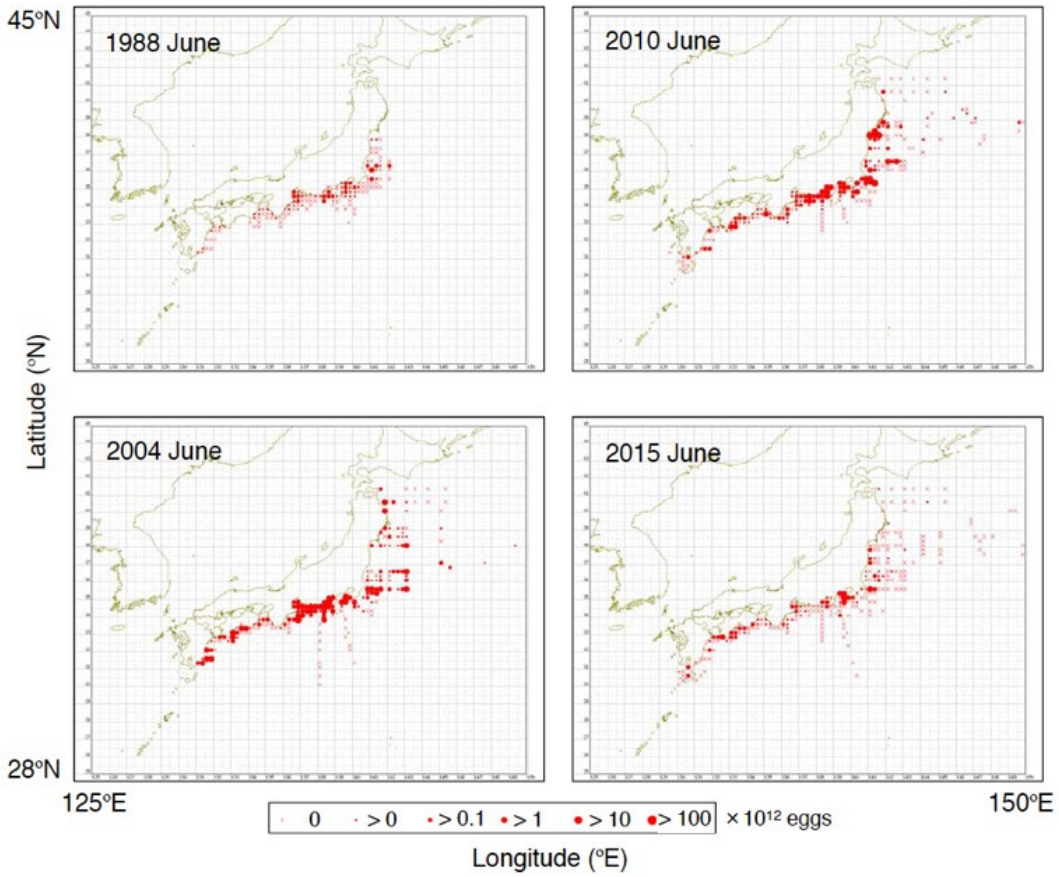

Figure R22-19. Monthly egg abundance distribution of Japanese anchovy (*Engraulis japonicus*) in June (main spawning month for anchovy) in 1988 (low-biomass period), 2004 (high-biomass period), 2010 (medium-biomass period), and 2015 (recent year). Monthly egg abundance was calculated by a combination of the mean egg density, survival rate, and egg incubation time at a 15' × 15' square level, based on an egg survey data set (Takasuka et al., 2008a).

Monthly egg abundance distributions for anchovy in June are shown in Figure R22-19. Anchovy spawn almost throughout the year with a peak in June to July. Their spawning grounds extend widely off the Pacific coast of Japan during the main spawning season. In 1988 (low-biomass period), anchovy spawned only in the inshore waters. In 2004 (high-biomass period), however, their spawning grounds expanded to the offshore waters. Their spawning was observed in the Kuroshio–Oyashio transition region up to 150°E. Anchovy still spawned intensively and widely in 2010 (medium-biomass period). In recent years (e.g. 2015), however, their spawning started to contract to the inshore waters. Spawning was not observed in the offshore waters > 145°E.

Pacific saury are also distributed and migrate over extensive areas of the Kuroshio Current system. Their eggs and larvae are transported and dispersed by the Kuroshio

Current (Oozeki et al., 2015). However, egg sampling is unable to quantify the egg distribution and abundance of Pacific saury because of the unique nature of their entangling eggs. Hence, a neuston net is towed at the sea surface to collect larvae and early juveniles of Pacific saury during the winter egg and larval surveys. In general, dense distributions of larvae and early juveniles are observed in areas around and on the offshore side of the Kuroshio axis except during a large Kuroshio meander year (Takasuka et al., 2014). Examples of distributions of larvae and early juveniles (< 50 mm knob length) during the winter spawning season are shown in Figure R22-10. In 2007 and 2010, larvae and early juveniles were densely distributed from the inshore to the offshore waters. As an exception, the distribution areas were relatively limited with lower densities in 2005 (a large Kuroshio meander year). During the last decade, however, the density of larvae and early juveniles has decreased, although the distribution areas did not dramatically change. This trend is still ongoing in response to the recent decline of Pacific saury biomass.

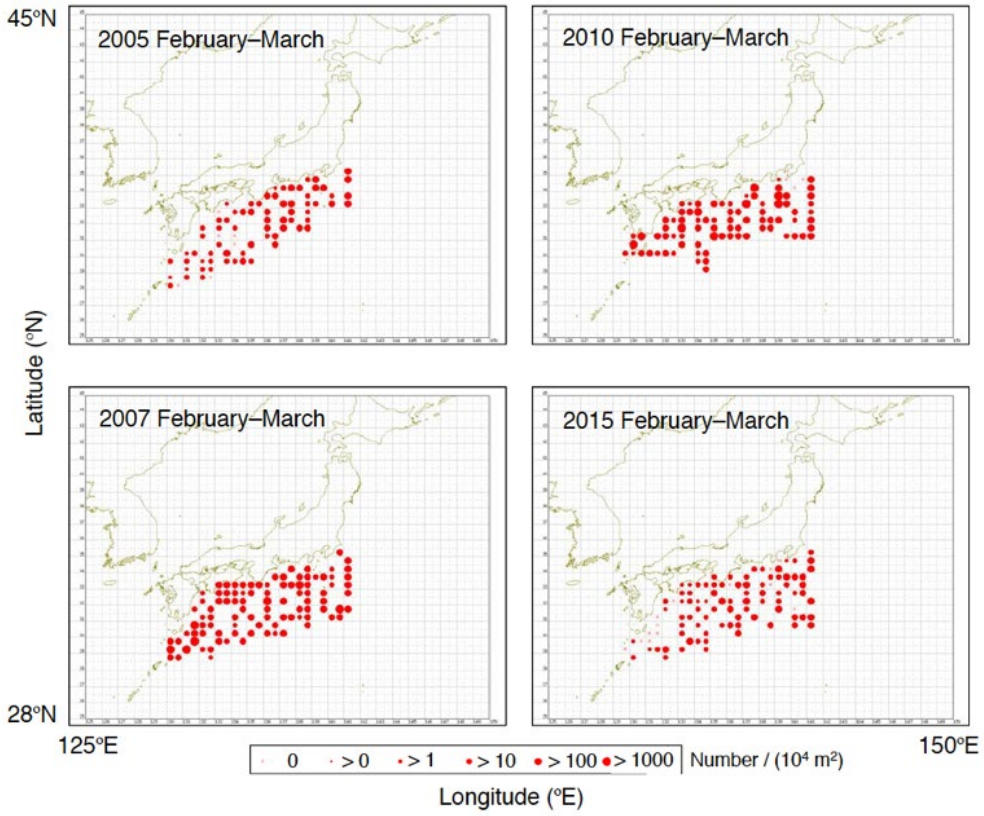

Figure R22-20. Horizontal distributions of Pacific saury (*Cololabis saira*) larvae and juveniles off the Pacific coast of Japan during February to March in 2005 (a large Kuroshio meander year), 2007, 2010, and 2015. Density was calculated as the number of individuals per swept area (individuals/10^4 m^2) for the individuals (<50 mm knob length). Modified and updated from Takasuka et al., (2014).

7.1.3. Mechanisms

Biological mechanisms underlying climate impacts on population dynamics of small pelagic fish include multiple processes, as recently reviewed for the Kuroshio Current system by Takasuka (2018). Food-based processes (i.e. trophodynamics) have been proposed in the Kuroshio Current system as well as upwelling systems. For example, there is a close relationship between the mortality coefficient anomaly from larval to age 1 sardine and the winter SST anomaly in the Kuroshio Extension and its southern recirculation area (Noto and Yasuda 1999). Based on this finding, a bottom-up hypothesis was proposed for sardine population dynamics. The hypothesis was supported by findings such that a deeper winter mixed layer leads to spring phytoplankton blooms in the nursery grounds for sardine (Nishikawa and Yasuda 2008; Nishikawa et al., 2011, 2013).

An alternative/complementary approach to the food-based hypotheses are temperature-based hypotheses. For example, differential optimal temperatures for growth rates during the early life stages between anchovy and sardine provide an explanation of species alternations under temperature fluctuations (Takasuka et al., 2007). Sardine and anchovy also have different optimal temperatures for spawning, which can switch advantage and disadvantage between the two species (Takasuka et al., 2008c, b). As well as food and temperature, intraspecific and interspecific interactions, fishing pressure, etc. could potentially influence the population dynamics of small pelagic fish.

Vital parameters such as growth and physiological conditions in fish are determined by a combination of environmental factors. In particular, growth rate during the early life stages has been used as a proxy for survival potential (Takasuka et al., 2017). The positive relationships of growth rate to recruitment success have been reported for several small pelagic species in the Kuroshio Current system and adjacent waters (e.g. Takahashi et al., 2008, 2012; Kamimura et al., 2015). As such, growth variability may be used as a predictor of recruitment success. However, the recruitment mechanisms may be different depending on the phases of population dynamics. As indicated in the time series of landing and estimated biomass, small pelagic fish are currently experiencing new phases of population dynamics in the Kuroshio Current system. The current situation may provide an opportunity to improve our understanding of mechanisms affecting their population dynamics.

7.2. Mesopelagic fishes

(Chiyuki Sassa)

In the world's oceans, mesopelagic fishes numerically dominate in fish assemblages, and have high biomasses. Global estimate of these fishes is in the order of ten billion tons (Irigoien et al., 2014), that is, about one hundred times the annual tonnage captured worldwide by commercial fishing. In the Kuroshio region off central and southern Japan (west of 150°E), the total mesopelagic fish biomass is estimated to be approximately from five to seven million tons (Gjøsæter and Kawaguchi 1980). However, this is considered to be underestimated, since it is based on data obtained by the towing of small-sized nets such as the ORI (Ocean Research Institute net) and IKMT (Isaacs-Kidd Midwater Trawl), from which a considerable number of medium- and large-sized specimens may escape (Pakhomov and Yamamura 2010). The biomass in the Kuroshio region would be potentially several times higher than the above estimate.

Micronektonic mesopelagic fishes are mainly composed of species belonging to the five families of Myctophidae, Gonostomatidae, Microstomatidae, Sternoptychidae, and Phosichthyidae. Myctophidae is the most speciose family and includes at least 248 species worldwide, 88 of which occur in the Kuroshio and its adjacent waters. Mesopelagic fishes act as an important link between secondary producers such as copepods and euphausiids and upper trophic levels in the oceanic ecosystem (Brodeur and Yamamura 2005). In the Kuroshio region, myctophids are a major prey item for commercially important pelagic and demersal fishes such as mackerels (*Scomber* spp.), splendid alfonsino (*Beryx splendens*), and bigeye tuna (*Thunnus obesus*). Also, they are consumed by cephalopods, sharks, and marine mammals such as common dolphins and pilot whales. Locally, myctophids such as *Diaphus suborbitalis*, *D. chrysorhynchus*, and *D. watasei* are consumed as human food in central and southern Japan, since they are sometimes incidentally caught in considerable numbers by set nets and shrimp trawls (Takagi 2017).

Oceanic species occur abundantly on the offshore side of the Kuroshio axis, while pseudoceanic species, adapting to certain habitats of continental slopes, slopes of islands, and seamounts, occur dominantly on the onshore side of the axis (Sassa et al., 2004; Ohshimo et al., 2012; Sassa and Konishi 2015). For example, juveniles of surface migratory myctophids showed three distinct patterns of horizontal distribution in relation to the Kuroshio axis. That is, pseudoceanic *Myctophum orientale* is restricted to the onshore side of the Kuroshio axis; *M. asperum* and *M. obtusirostre* occur mainly along the Kuroshio frontal area; and *Centrobranchus nigroocellatus*, *Hygophum reinhardtii*, and *Symbolophorus evermanni* on the offshore side of the axis (Sassa, unpublished data).

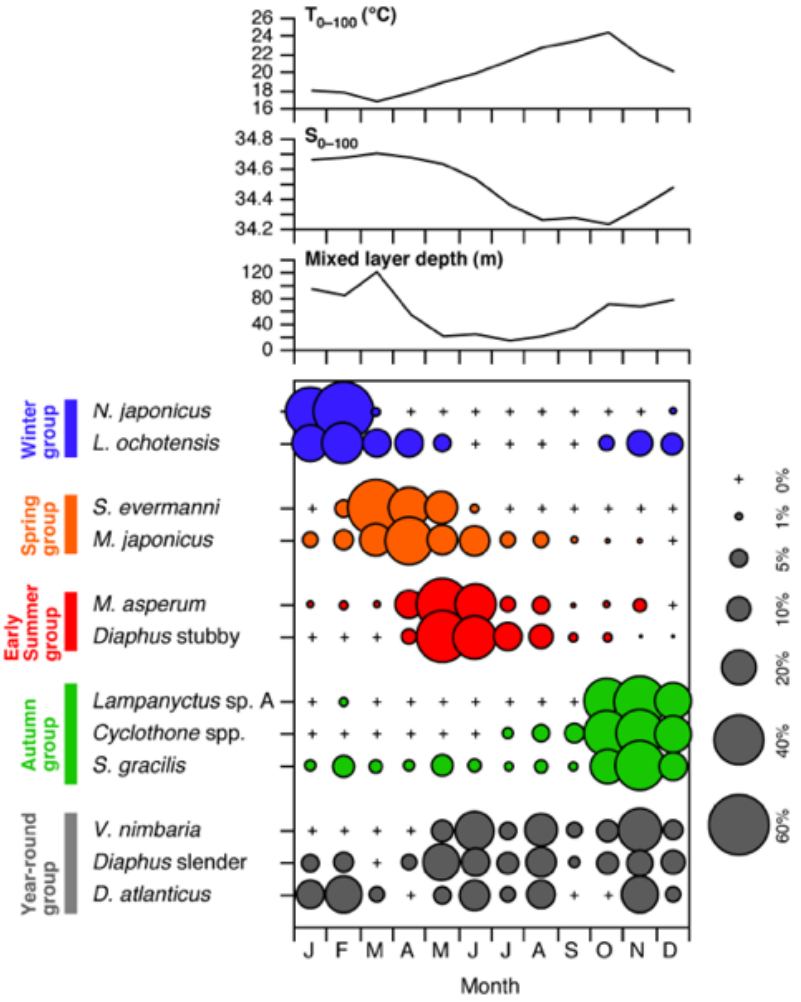

Figure R22-21. Seasonal occurrence patterns of the larvae of the twelve dominant mesopelagic fish species on the continental slope in Tosa Bay, Shikoku. Each value is the monthly mean abundance between 2001 and 2004, expressed as a percentage of the total catch. Monthly changes in mean temperature and salinity over the 0–100 m depth ($T_{0–100}$ and $S_{0–100}$, respectively) and mixed layer depth are also shown. Modified from (Sassa and Hirota 2013).

Various species of mesopelagic fishes, including several subarctic and transitional water species, use the Kuroshio region as spawning and nursery grounds. To describe the reproductive seasonality, seasonal occurrence patterns of mesopelagic fish larvae were examined on the continental slope off southern Japan, which is strongly influenced by the Kuroshio (Sassa and Hirota 2013). The seasonal occurrence patterns of the twelve most abundant larvae were categorized into five groups (Figure R22-21), Winter (*Notoscopelus japonicus* and *Lipolagus ochotensis*); Spring (*Symbolophorus evermanni* and *Maurolicus japonicus*); Early summer (*Myctophum asperum* and *Diaphus* stubby type); Autumn (*Lampanyctus* sp. A, *Cyclothone* spp., and *Sigmops*

gracilis); and Year-round (*Vinciguerria nimbaria*, *Diaphus* slender type, and *Diogenichthys atlanticus*) groups. No significant difference was observed in the months of peak abundances of these larvae during 2001 to 2004, suggesting that each species has a fixed seasonal pattern of reproduction.

Reproductive characteristics of adults of four dominant pseudoceanic myctophids (*Benthosema pterotum*, *Diaphus chrysorhynchus*, *D. garmani*, and *D. watasei*) were investigated off southern Japan (Sassa et al., 2014, 2016). There were more females than males in the overall catches, and the ratio of females to males increased with standard length (SL). Based on diel occurrence pattern of females with hydrated ovaries, spawning is considered to occur in the mesopelagic layer during or shortly after dusk. Oocytes at various sizes were found in mature ovaries, indicating that females are multiple spawners, with spawning frequencies of approximately 3–9 days. Mean egg size at hydration was smallest in *D. garmani* (0.60 mm) and largest in *B. pterotum* (0.71 mm). Batch fecundity of average-sized mature females was lowest in *B. pterotum* (1200 eggs at 47 mm SL) and highest in *D. watasei* (23200 eggs at 147 mm SL).

High abundances of mesopelagic fish larvae are observed in the Kuroshio region throughout the year. Recently, the growth and mortality of six numerically dominant mesopelagic fish larvae in winter were examined (Figure R22-22; Sassa and Takahashi 2018). The weight-specific growth coefficient ranged from 0.08 (*Sigmops gracilis*) to 0.16 d^{-1} (*Vinciguerria nimbaria*), and the instantaneous daily mortality coefficient from 0.07 (S. *gracilis*) to 0.14 d^{-1} (*Myctophum asperum*). The growth rate of the mesopelagic fish larvae based on sagittal otolith microstructure was approximately one half to one third of the growth of the small pelagic fish larvae of Japanese sardine (*Sardinops melanostictus*), spotted mackerel (*Scomber australasicus*), and Japanese jack mackerel (*Trachurus japonicus*) in the Kuroshio region during winter. This corresponded with the findings that the growth rates of the juveniles and adults of the mesopelagic fishes are lower than those of small pelagic fishes (Takagi et al., 2006).

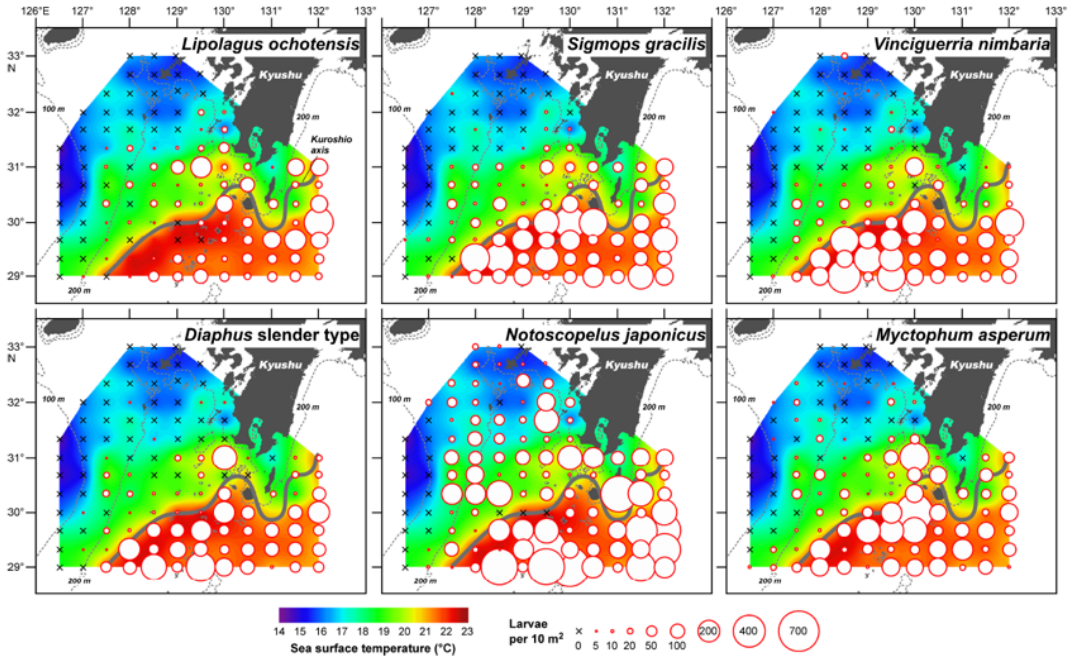

Figure R22-22. Horizontal distributions of the six numerically dominant mesopelagic fish larvae off southwestern Kyushu Island in February 2010. The color contours indicate sea surface temperature (°C). Circles represent the abundance as a continuous range of values >0. Crosses indicate no catch. Modified from Sassa and Takahashi (2018).

There has been interest in the predatory impact of vertically migrating mesopelagic fishes on zooplankton in the western North Pacific. In the Kuroshio region during winter, Watanabe et al., (2002) estimated that food requirements of juveniles of four surface migratory myctophids are 0.2–4.6 mg C m^{-2} d^{-1} in the surface layer at night, with a predatory impact on zooplankton biomass of 0.9–10.9%. Food requirements of adults of *Diaphus garmani* and *D. chrysorhynchus* were 32.7 mg C m^{-2} d^{-1} in the slope region off southern Japan during summer, and the predatory impact of the two species on zooplankton production was estimated to be 47–92% and 7–14%, respectively (Tanaka et al., 2013). Recently, food requirements of six numerically dominant mesopelagic fish larvae (Figure R22-22) were estimated to be 1.4 mg C m^{-2} d^{-1} in the Kuroshio region during winter (Sassa and Takahashi 2018). The predatory impact of the larvae on the production rate of the available prey was estimated to be approximately 3.5–5.3%, implying that the larvae have a low level but consistent effect on zooplankton production in the Kuroshio region.

In the Kuroshio region during winter, decadal change in juvenile abundance of surface migratory myctophid fishes was examined by Watanabe and Kawaguchi (2003) for a period of 35 years from 1957 to 1994. They showed substantial interannual variability and decadal-scale trends in some species. To update this time series, re-analysis of

specimens collected in the surface layer at night from 2000 to the present is progressing. In the preliminary results, several tropical species have tended to show an increasing trend after 2000, which is possibly related to the increasing trend in water temperature in the Kuroshio region (Sassa 2019). In the future, detailed investigations on time series of myctophid juveniles need to be conducted in relation to large-scale physical and biological oceanographic changes.

8. References

Barange, M., Coetzee, J., Takasuka, A., and Hill, K. 2009. Habitat expansion and contraction in anchovy and sardine populations. Prog. Oceanogr 83: 251–260, doi:10.1016/j.pocean.2009.07.027

Brodeur, R.D. and Yamamura, O. 2005. Micronekton of the North Pacific. PICES Sci Rep. 30, 115 pp.

Ceballos, L.I., Di Lorenzo, E., Hoyos, C.D., Schneider, N., and Taguchi, B. 2009. North Pacific Gyre Oscillation synchronizes climate fluctuations in the eastern and western boundary systems. J. Clim. 22: 5163–5174, doi: 10.1175/2009JCLI2848.1

Chavez, F.P., Ryan, J., Lluch-Cota, S.E., and Niquen, C.M. 2003. From anchovies to sardines and back, multidecadal change in the Pacific Ocean. Science 299: 217–221, doi:10.1126/science.1075880

Chen, S.-J,, Kuo, Y.-H., Zhang, P.-Z., and Bai, Q.-F. 2002. Climatology of Explosive Cyclones off the East Asian Coast. Mon. Wea. Rev. 120,3029–120,3035, doi:10.1175/1520-0493(1992)120<3029,coecot>2.0.co;2

Davis, R.E. 1976. Predictability of sea surface temperature and sea level pressure anomalies over the North Pacific Ocean. J. Phys. Oceanogr. 6: 249–266, doi:10.1175/1520-0485(1976)006<0249,POSSTA>2.0.CO;2

Deser, C., Alexander, M.A., and Timlin, M.S. 1999. Evidence for a wind-driven intensification of the Kuroshio Current extension from the 1970s to the 1980s. J. Clim. 12,1697–12,1706, doi:10.1175/1520-0442(1999)012<1697,EFAWDI>2.0.CO;2

Endoh, T. and Hibiya, T. 2001. Numerical simulation of the transient response of the Kuroshio leading to the large meander formation south of Japan. J. Geophys. Res. Oceans 106: 26,833–26,850, doi:10.1029/2000JC000776

Endoh, T., Tsujino, H., and Hibiya, T. 2011. The effect of Koshu Seamount on the formation of the Kuroshio large meander south of Japan. J. Phys. Oceanogr. 41: 1624–1629, doi:10.1175/JPO-D-11-074.1

FRA (Japan Fisheries Research and Education Agency). 2017. Marine fisheries stock assessment and evaluation for Japanese waters. fiscal year 2016/2017. Tokyo and Yokohama

Frankignoul, C. 1985. Sea surface temperature anomalies, planetary waves, and air-sea feedback in the middle latitudes. Rev. Geophys. 23: 357, doi:10.1029/RG023i004p00357

Frankignoul, C. and Kestenare, E. 2002. The surface heat flux feedback. Part I, estimates from observations in the Atlantic and the North Pacific. Clim. Dyn. 19: 633–647, doi:10.1007/s00382-002-0252-x

Gjøsæter, J. and Kawaguchi, K. 1980. A review of the world resources of mesopelagic fish. FAO Fish. Tech. Pap. 193, pp. 1–151.

Gyakum, J.R., Anderson, J.R., Grumm, R.H., and Gruner, E.L. 1989. North Pacific cold-season surface cyclone activity, 1975–1983. Mon. Wea. Rev. 117: 1141–1155, doi:10.1175/1520-0493(1989)117<1141,NPCSSC>2.0.CO;2

Hayasaki, M., Kawamura, R., Mori, M., and Watanabe, M. 2013. Response of extratropical cyclone activity to the Kuroshio large meander in northern winter. Geophys. Res. Lett. 40: 2851–2855, doi:10.1002/grl.50546

Hidaka, K. and Nakata, K. 2010. Interannual variations of the planktonic ecosystem in the slope water and Kuroshio south of Japan in February in the years 1990–2002. J. Oceanogr. 66: 741–753, doi:10.1007/s10872-010-0061-5

Hirai, J., Hidaka, K., Nagai, S., and Ichikawa, T. 2017. Molecular-based diet analysis of the early post‐larvae of Japanese sardine *Sardinops melanostictus* and Pacific round herring *Etrumeus teres*. Mar. Ecol. Prog. Ser. 564: 99–113, doi:10.3354/meps12008

Hirata, H., Kawamura, R., Kato, M., and Shinoda, T. 2015. Influential role of moisture supply from the Kuroshio/Kuroshio Extension in the rapid development of an extratropical cyclone. Mon. Wea. Rev. 143: 4126–4144, doi:10.1175/MWR-D-15-0016.1

Ichikawa, T., Segawa, K., Morita, H., and Tanaka, T. 2009. Usefulness of bench-top VPR(B-VPR. in measuring formalin-preserved zooplankton samples. J. Fish. Technol. 1: 13–23.

Iizuka, S., Shiota, M., Kawamura, R., and Hatsushika, H. 2013. Influence of the monsoon variability and sea surface temperature front on the explosive cyclone activity in the vicinity of Japan during northern winter. SOLA 9: 1–4, doi:10.2151/sola.2013-001

Irigoien, X., Klevjer, T.A., Røstad, A., Martinez, U., Boyra, G., Acuña, J.L., Bode, A., Echevarria, F., Gonzalez-Gordillo, J.I., Hernandez-Leon, S., Agusti, S., Aksnes, D.L., Duarte, C.M., and Kaartvedt, S. 2014. Large mesopelagic fishes biomass and trophic efficiency in the open ocean. Nat. Commun. 5: 3271, doi:10.1038/ncomms4271

Itoh, S., Yasuda, I. 2010. Characteristics of mesoscale eddies in the Kuroshio–Oyashio

Extension region detected from the distribution of the sea surface height anomaly. J. Phys. Oceanogr. 40: 1018–1034, doi:10.1175/2009JPO4265.1

Iwao, K., Inatsu, M., and Kimoto, M. 2012. Recent changes in explosively developing extratropical cyclones over the winter northwestern Pacific. J. Clim. 25: 7282–7296, doi:10.1175/JCLI-D-11-00373.1

Iwasaka, N., Hanawa, K., and Toba Y. 1987. Analysis of SST anomalies in the North Pacific and their relation to 500mb height anomalies over the Northern Hemisphere during 1969-1979. J. Meteorol. Soc. Japan Ser. II 65: 103–114, doi:10.2151/jmsj1965.65.1_103

Joyce, T.M., Kwon, Y.-O., and Yu, L. 2009. On the relationship between synoptic wintertime atmospheric variability and path shifts in the Gulf Stream and the Kuroshio Extension. J. Clim. 22: 3177–3192, doi:10.1175/2008JCLI2690.1

Kamimura, Y., Takahashi, M., Yamashita N, Watanabe, C., and Kawabata, A. 2015. Larval and juvenile growth of chub mackerel *Scomber japonicus* in relation to recruitment in the western North Pacific. Fish. Sci. 81: 505–513, doi:10.1007/s12562-015-0869-4

Kawabe, M. 1987. Spectral properties of sea level and time scales of Kuroshio path variations. J. Oceanogr, Soc. Japan 43: 111–123, doi:10.1007/BF02111887

Kawabe, M. 1985. Sea level variations at the Izu Islands and typical stable paths of the Kuroshio. J. Oceanogr. Soc. Japan 41: 307–326, doi:10.1007/BF02109238

Kawai, H. 1969. Statistical estimation of isotherms indicative of the Kuroshio axis. Deep Sea Res. 16(Suppl.),109–115

Kawai, Y., Miyama, T., Iizuka, S., Manda, A., Yoshioka, M.Y., Katagiri, S., Tachibana, Y. and Nakamura, H. 2015. Marine atmospheric boundary layer and low-level cloud responses to the Kuroshio Extension front in the early summer of 2012: three-vessel simultaneous observations and numerical simulations. J. Oceanogr. 71: 511–526, doi:10.1007/s10872-014-0266-0

Kawakami, Y., Sugimoto, S., and Suga, T. 2016. Inter-annual zonal shift of the formation region of the lighter variety of the North Pacific Central Mode Water. J. Oceanogr 72: 225–234, doi:10.1007/s10872-015-0325-1

Kawasaki, T. 1983. Why do some pelagic fishes have wide fluctuations in their numbers? Biological basis of fluctuation from the viewpoint of evolutionary ecology. FAO Fish. Rep. 291, pp. 1065–1080.

Kidachi, T., and Ito, H. 1979. Distribution and structure of macroplankton communities in the Kuroshio and coastal region, south of Honshu, during spring season.

Bull. Tokai Reg. Fish. Res. Lab. 97: 1–119.

Kodama, T., Shimizu, Y., Ichikawa, T., Hiroe, Y., Kusaka, A., Morita, H., Shimizu, M. and Hidaka, K. 2014. Seasonal and spatial contrast in the surface layer nutrient content around the Kuroshio along 138°E, observed between 2002 and 2013. J. Oceanogr. 70: 489–503, doi:10.1007/s10872-014-0245-5

Kouketsu, S., Tomita, H., Oka, E., Hosoda, S., Kobayashi, T., and Sato, K. 2012. The role of meso-scale eddies in mixed layer deepening and mode water formation in the western North Pacific. J. Oceanogr. 68: 63–77, doi:10.1007/s10872-011-0049-9

Kuwano-Yoshida, A., Asuma, Y. 2008. Numerical study of explosively developing extratropical cyclones in the northwestern Pacific region. Mon. Wea. Rev. 136: 712–740, doi:10.1175/2007MWR2111.1

Kuwano-Yoshida, A., Minobe, S. 2017. Storm-track response to SST fronts in the northwestern Pacific region in an AGCM. J. Clim. 30: 1081–1102, doi:10.1175/JCLI-D-16-0331.1

Kwon, Y.-O., Alexander, M.A., Bond, N.A., Frankignoul, C., Nakamura, H. Qiu, B., and Thompson, L.A. 2010. Role of the Gulf Stream and Kuroshio–Oyashio systems in large-scale atmosphere–ocean interaction: A review. J. Clim. 23: 3249–3281, doi:10.1175/2010JCLI3343.1

Lluch-Belda, D., Crawford, R.J.M., Kawasaki, T., MacCall, A.D., Parrish, R.H., Schwartzlose, R.A., and Smith, P.E. 1989. World-wide fluctuations of sardine and anchovy stocks: the regime problem. S. African J. Mar. Sci. 8,195–205. doi:10.2989/02577618909504561

Mantua, N.J. and Hare, S.R. 2002. The Pacific Decadal Oscillation. J. Oceanogr. 58: 35–44, doi:10.1023/A,1015820616384

Masunaga, R., Nakamura, H., Miyasaka, T., Nishii, K., and Tanimoto, Y. 2015. Separation of climatological imprints of the Kuroshio Extension and Oyashio fronts on the wintertime atmospheric boundary layer: Their sensitivity to SST resolution prescribed for atmospheric reanalysis. J. Clim. 28 : 1764–1787, doi:10.1175/JCLI-D-14-00314.1

Masunaga, R., Nakamura, H., Miyasaka, T., Nishii, K. and Qiu, B. 2016. Interannual modulations of oceanic imprints on the wintertime atmospheric boundary layer under the changing dynamical regimes of the Kuroshio Extension. J. Clim. 29 : 3273–3296, doi:10.1175/JCLI-D-15-0545.1

Matsumura, S., Horinouchi, T., Sugimoto, S., and Sato, T. 2016. Response of the baiu

rainband to northwest Pacific SST anomalies and its impact on atmospheric circulation. J. Clim. 29: 3075–3093, doi:10.1175/JCLI-D-15-0691.1

Miller, A.J., Cayan, D.R., and White, W.B. 1998. A westward-intensified decadal change in the North Pacific thermocline and gyre-scale circulation. J. Clim. 11: 3112–3127, doi:10.1175/1520-0442(1998)011<3112,AWIDCI>2.0.CO;2

Miyamoto, H., Itoh, H., and Okazaki, Y. 2017. Temporal and spatial changes in the copepod community during the 1974–1998 spring seasons in the Kuroshio region; a time period of profound changes in pelagic fish populations. Deep Sea Res. 128: 131–140, doi:10.1016/J.DSR.2017.07.007

Murazaki, K., Tsujino, H., Tatsuo, M., and Kurihara, K. 2015. Influence of the Kuroshio Large Meander on the climate around Japan based on a regional climate model. J. Meteorol. Soc. Japan Ser. II 93: 161–179, doi:10.2151/jmsj.2015-009

Nakamura, H., Nishina, A., and Minobe S. 2012. Response of storm tracks to bimodal Kuroshio path states south of Japan. J. Clim. 25: 7772–7779, doi:10.1175/JCLI-D-12-00326.1

Nakamura, H., Sampe, T., Tanimoto, Y., and Shimpo, A. 2004a. Observed associations among storm tracks, jet streams and midlatitude oceanic fronts. In, Wang, C., Xie, S.P., Carton, J.A., eds. Earth's Climate: The Ocean-Atmosphere Interaction, Vol. 147, Geophys. Monogr. Ser., AGU, pp. 329–345, doi: 10.1029/147GM18

Nakamura, H., Shimpo, A., Nakamura, H., and Shimpo, A. 2004b. Seasonal variations in the Southern Hemisphere storm tracks and jet streams as revealed in a reanalysis dataset. J. Clim. 17: 1828–1844, doi:10.1175/1520-0442(2004)017<1828,SVITSH>2.0.CO;2

Nakata, K. and Hidaka, K. 2003. Decadal-scale variability in the Kuroshio marine ecosystem in winter. Fish. Oceanogr. 12: 234–244, doi:10.1046/j.1365-2419.2003.00249.x

Nakata, K. and Koyama, S. 2003. Interannual changes of the winter to early spring biomass and composition of mesozooplankton in the Kuroshio region in relation to climatic factors. J. Oceanogr. 59: 225–234, doi:10.1023/A,1025547406567

NGDC (National Geophysical Data Center). 2006. 2-minute Gridded Global Relief Data (ETOPO2v2) https,//www.ngdc.noaa.gov/mgg/global/etopo2.html. Accessed 16 Apr 2019

Nishikawa, H., Tachibana, Y., Kawai, Y., Yoshioka, M.K. and Nakamura, H. 2016. Evidence for SST-forced anomalous winds revealed from simultaneous radiosonde launches from three ships across the Kuroshio Extension front. Mon. Wea. Rev. 144: 3553–3567, doi:10.1175/MWR-D-15-0442.1

Nishikawa, H. and Yasuda, I. 2008. Japanese sardine (*Sardinops melanostictus*) mortality in relation to the winter mixed layer depth in the Kuroshio Extension region. Fish. Oceanogr. 17: 411–420, doi:10.1111/j.1365-2419.2008.00487.x

Nishikawa, H., Yasuda, I., and Itoh, S. 2011. Impact of winter-to-spring environmental variability along the Kuroshio jet on the recruitment of Japanese sardine. *Sardinops melanostictus*. Fish. Oceanogr. 20: 570–582, doi:10.1111/j.1365-2419.2011.00603.x

Nishikawa, H., Yasuda, I., Komatsu, K., Sasaki, H., Sasai, Y., Setou, T., and Shimizu, M. 2013. Winter mixed layer depth and spring bloom along the Kuroshio front: Implications for the Japanese sardine stock. Mar. Ecol. Prog. Ser. 487: 217–229, doi:10.3354/meps10201

Nonaka, M., Nakamura, H., Tanimoto, Y., Kagimoto, T., and Sasaki, H. 2006. Decadal variability in the Kuroshio–Oyashio Extension simulated in an eddy-resolving OGCM. J. Clim. 19: 1970–1989, doi:10.1175/JCLI3793.1

Nonaka, M. and Xie, S.-P. 2003. Covariations of sea surface temperature and wind over the Kuroshio and its extension: Evidence for ocean-to-atmosphere feedback. J. Clim. 16: 1404–1413, doi:10.1175/1520-0442(2003)16<1404,COSSTA>2.0.CO;2

Noto, M. and Yasuda, I. 1999. Population decline of the Japanese sardine, *Sardinops melanostictus*, in relation to sea surface temperature in the Kuroshio Extension. Can. J. Fish. Aquat. Sci. 56: 973–983, doi:10.1139/f99-028

Ohshimo, S., Yasuda, T., Tanaka, H., and Sassa, C. 2012. Biomass fluctuation of two dominant lanternfish *Diaphus garmani* and *D. chrysorhynchus* with environmental changes in the East China Sea. Fish. Sci. 78: 33–39, doi: 10.1007/s12562-011-0424-x

Oka, E., Qiu, B., Kouketsu, S., Uehara, K., and Suga, T. 2012. Decadal seesaw of the Central and Subtropical Mode Water formation associated with the Kuroshio Extension variability. J. Oceanogr. 68,355–360, doi: 10.1007/s10872-011-0098-0

Okazaki, Y., Tadokoro, K., Kubota, H., Kamimura, Y., and Hidaka, K. 2019. Dietary overlap and optimal prey environments of larval and juvenile sardine and anchovy in the mixed water region of the western North Pacific. Mar. Ecol.

Prog. Ser. 630: 149–160, doi:10.3354/meps13124

Ono, T., Kodama, T., Shimizu, Y., et al., 2015. Long-term variability of nutricline depth in the winter Kuroshio slope area. Abstr. 2015 Autumn Meet Japan Oceanogr Soc 327

Oozeki, Y., Okunishi, T., Takasuka, A., and Ambe, D. 2015. Variability in transport processes of Pacific saury *Cololabis saira* larvae leading to their broad dispersal: Implications for their ecological role in the western North Pacific. Prog. Oceanogr. 138: 448–458, doi:10.1016/J.POCEAN.2014.05.011

Oozeki, Y., Takasuka, A., Kubota, H., and Barange, M. 2007. Characterizing spawning habitats of Japanese sardine (*Sardinops melanostictus*), Japanese anchovy (*Engraulis japonicas*), and Pacific round herring (*Etrumeus teres*) in the northwestern Pacific. Calif. Coop. Ocean. Fish. Investig. Rep. 48: 191–203.

Pakhomov, E. and Yamamura, O. eds. 2010. Report of the Advisory Panel on Micronekton Sampling Inter-calibration Experiment. PICES Sci Rep 38, 115 pp.

Qiu, B. and Chen, S. 2010. Eddy-mean flow interaction in the decadally modulating Kuroshio Extension system. Deep Sea Res II 57: 1098–1110, doi:10.1016/J.DSR2.2008.11.036

Qiu, B., Chen, S., and Hacker, P. 2007. Effect of mesoscale eddies on Subtropical Mode Water variability from the Kuroshio Extension System Study. KESS.. J. Phys. Oceanogr. 37: 982–1000, doi:10.1175/JPO3097.1

Qiu, B., Chen, S. 2005. Variability of the Kuroshio Extension jet, recirculation gyre, and mesoscale eddies on decadal time scales. J. Phys. Oceanogr. 35: 2090–2103, doi:10.1175/JPO2807.1

Qiu, B., Chen, S. 2006. Decadal variability in the formation of the North Pacific Subtropical Mode Water: Oceanic versus atmospheric control. J. Phys. Oceanogr. 36: 1365–1380, doi:10.1175/JPO2918.1

Qiu, B., Chen, S., Schneider, N., and Taguchi, B. 2014. A coupled decadal prediction of the dynamic state of the Kuroshio Extension system. J. Clim. 27: 1751–1764, doi:10.1175/JCLI-D-13-00318.1

Qiu B., 2003. Kuroshio Extension variability and forcing of the Pacific decadal oscillations: Responses and potential feedback. J. Phys. Oceanogr. 33: 2465–2482, doi:10.1175/2459.1

Ren, L. and Riser, S.C. 2010. Observations of decadal time scale salinity changes in the subtropical thermocline of the North Pacific Ocean. Deep Sea Res II 57:

1161–1170, doi:10.1016/j.dsr2.2009.12.005

Reynolds, R.W., Smith, T.M., Liu, C., Chelton, D.B., Casey, K.S. and Schlax, M.G. 2007. Daily high-resolution-blended analyses for sea surface temperature. J. Clim. 20: 5473–5496, doi:10.1175/2007JCLI1824.1

Sakamoto, T.T., Hasumi, H., Ishii, M., Emori, S., Suzuki, T., Nishimura, T., and Sumi, A. 2005. Responses of the Kuroshio and the Kuroshio Extension to global warming in a high-resolution climate model. Geophys. Res. Lett. 32, doi: 10.1029/2005GL023384

Sasaki, Y.N. and Minobe, S. 2015. Climatological mean features and interannual to decadal variability of ring formations in the Kuroshio Extension region. J. Oceanogr. 71: 499–509, doi:10.1007/s10872-014-0270-4

Sassa, C. 2019. Reproduction and early life history of mesopelagic fishes in the Kuroshio region, a review of recent advances. In, Nagai, T., Saito, H., Suzuki, K., Takahashi, M., eds. Kuroshio Current, Physical, Biogeochemical, and Ecosystem Dynamics. Geophys. Monogr. Ser., AGU, pp. 273–294.

Sassa, C. and Hirota, Y. 2013. Seasonal occurrence of mesopelagic fish larvae on the onshore side of the Kuroshio off southern Japan. Deep Sea Res. 81: 49–61, doi:10.1016/J.DSR.2013.07.008

Sassa, C., Kawaguchi, K., Hirota, Y. and Ishida, M. 2004. Distribution patterns of larval myctophid fish assemblages in the subtropical-tropical waters of the western North Pacific. Fish. Oceanogr. 13: 267–282, doi: 10.1111/j.1365-2419.2004.00289.x

Sassa, C. and Konishi, Y. 2015. Late winter larval fish assemblage in the southern East China Sea, with emphasis on spatial relations between mesopelagic and commercial pelagic fish larvae. Cont. Shelf Res. 108: 97–111, doi: 10.1016/J.CSR.2015.08.021

Sassa, C., Ohshimo, S., Tanaka, H. and Tsukamoto, Y. 2014. Reproductive biology of *Benthosema pterotum* (Teleostei: Myctophidae) in the shelf region of the East China Sea. J. Mar. Biol. Assoc. UK 94: 423–433, doi: 10.1017/S0025315413001318

Sassa, C. and Takahashi, M. 2018. Comparative larval growth and mortality of mesopelagic fishes and their predatory impact on zooplankton in the Kuroshio region. Deep Sea Res. 131: 121–132, doi:10.1016/J.DSR.2017.11.007

Sassa, C., Tanaka, H. and Ohshimo, S. 2016. Comparative reproductive biology of three dominant myctophids of the genus *Diaphus* on the slope region of the

East China Sea. Deep Sea Res. 115: 145–158, doi: 10.1016/J.DSR.2016.06.005

Schneider, N., Miller, A.J., and Pierce, D.W. 2002. Anatomy of North Pacific decadal variability. J. Clim. 15: 586–605. doi: 10.1175/1520-0442(2002)015<0586,AONPDV>2.0.CO;2

Seager, R., Kushnir, Y., Naik, N.H., Cane, M.A., and Miller, J. 2001. Wind-driven shifts in the Latitude of the Kuroshio–Oyashio Extension and generation of SST anomalies on decadal timescales. J. Clim. 14: 4249–4265, doi: 10.1175/1520-0442(2001)014<4249,WDSITL>2.0.CO;2

Seo, Y., Sugimoto, S., and Hanawa, K. 2014. Long-term variations of the Kuroshio Extension path in winter: Meridional movement and path state change. J. Clim. 27: 5929–5940, doi:10.1175/JCLI-D-13-00641.1

Sogawa, S., Hidaka, K., Kamimura, Y., Takahashi, M., Saito, H., Okazaki, Y., Shimizu, Y., and Setou, T. 2019. Environmental characteristics of spawning and nursery grounds of Japanese sardine and mackerels in the Kuroshio and Kuroshio Extension area. Fish. Oceanogr. 28 : 454–467, doi:10.1111/fog.12423

Sogawa, S., Kidachi, T., Nagayama, M., Ichikawa, T., Hidaka, K., Ono, T., and Shimizu, Y. 2017. Short-term variation in copepod community and physical environment in the waters adjacent to the Kuroshio Current. J. Oceanogr 73: 603–622, doi: 10.1007/s10872-017-0420-6

Sugimoto, S., Aono, K., and Fukui, S. 2017. Local atmospheric response to warm mesoscale ocean eddies in the Kuroshio–Oyashio Confluence region. Sci. Rep. 7: 11871, doi:10.1038/s41598-017-12206-9

Sugimoto, S. and Hanawa, K. 2012. Relationship between the path of the Kuroshio in the south of Japan and the path of the Kuroshio Extension in the east. J. Oceanogr 68: 219–225, doi:10.1007/s10872-011-0089-1

Sugimoto, S. and Hanawa, K. 2009. Decadal and interdecadal variations of the Aleutian Low activity and their relation to upper oceanic variations over the North Pacific. J. Meteorol. Soc. Japan 87,601–87,614, doi:10.2151/jmsj.87.601

Sugimoto, S., Hanawa, K. 2011. Roles of SST Anomalies on the wintertime turbulent heat fluxes in the Kuroshio–Oyashio Confluence Region: Influences of warm eddies detached from the Kuroshio Extension. J. Clim. 24: 6551–6561, doi:10.1175/2011JCLI4023.1

Sugimoto, S. and Kako, S. 2016. Decadal variation in winter mixed layer depth south of the Kuroshio Extension and its influence on winter mixed layer temperature. J. Clim, 29: 1237–1252, doi: 10.1175/JCLI-D-15-0206.1

Sugimoto, S. 2014. Influence of SST anomalies on winter turbulent heat fluxes in the eastern Kuroshio–Oyashio confluence region. J. Clim. 27: 9349–9358, doi:10.1175/JCLI-D-14-00195.1

Sugisaki, H. 2010. Status and trends of the Kuroshio region, 2003–2008. In, Mckinnell SM, Dagg MJ. eds. Marine Ecosystems of the North Pacific Ocean 2003-2008. PICES Special Publication Number 4, pp. 330–359.

Taguchi, B., Xie, S.-P., Mitsudera, H., and Kubokawa, A. 2005. Response of the Kuroshio Extension to Rossby waves associated with the 1970s climate regime shift in a high-resolution ocean model. J. Clim. 18: 2979–2995, doi: 10.1175/JCLI3449.1

Taguchi, B., Xie, S.-P., Schneider, N., Nonaka, M., Sasaki, and Sasai, Y. 2007. Decadal variability of the Kuroshio Extension: Observations and an eddy-resolving model hindcast. J. Clim. 20: 2357–2377, doi, 10.1175/JCLI4142.1

Takagi, K., Yatsu, A., Itoh, H., and Moku, M. 2009. Comparison of feeding habits of myctophid fishes and juvenile small epipelagic fishes in the western North Pacific. Mar. Biol .156: 641–659, doi:10.1007/s00227-008-1115-8

Takagi, K., Yatsu, A., Moku, M., and Sassa, C. 2006. Age and growth of lanternfishes, *Symbolophorus californiensis* and *Ceratoscopelus warmingii* (Myctophidae), in the Kuroshio–Oyashio Transition Zone. Ichthyol. Res. 53: 281–289, doi: 10.1007/s10228-006-0346-2

Takagi, T. 2017. *Diaphus suborbitalis* to the table - Recent activities at the Shizuoka Prefectural Research Institute of Fishery. Nippon Suisan Gakkaishi 83: 697.

Takahashi, H.G., Adachi, S.A., Sato, T., Hara, M., Ma, X, and Kimura, F. 2015. An oceanic impact of the Kuroshio on surface air temperature on the Pacific coast of Japan in summer: Regional H_2O greenhouse gas effect. J. Clim. 28: 7128–7144. doi:10.1175/JCLI-D-14-00763.1

Takahashi, M., Nishida, H., Yatsu, A. and Watanabe, Y. 2008. Year-class strength and growth rates after metamorphosis of Japanese sardine (*Sardinops melanostictus*) in the western North Pacific Ocean during 1996–2003. Can. J. Fish. Aquat. Sci. 65: 1425–1434, doi:10.1139/F08-063

Takahashi, M., Sassa, C., and Tsukamoto, Y. 2012. Growth-selective survival of young jack mackerel *Trachurus japonicus* during transition from pelagic to demersal

habitats in the East China Sea. Mar. Biol. 159: 2675–2685, doi: 10.1007/s00227-012-2025-3

Takasuka, A. 2018. Biological mechanisms underlying climate impacts on population dynamics of small pelagic fish. In, Aoki, I., Yamakawa, T., Takasuka, A. eds. Fish Population Dynamics, Monitoring, and Management. Springer, Japan, pp. 19–50.

Takasuka, A., Kubota, H., and Oozeki, Y. 2008a. Spawning overlap of anchovy and sardine in the western North Pacific. Mar. Ecol. Prog. Ser. 366: 231–244, doi: 10.3354/meps07514

Takasuka, A., Kuroda, H., Okunishi, T., Shimizu, Y., Hirota, Y., Kubota, H., Sakaji, H., Kimura, R., Ito, S.I. and Oozeki, Y. 2014. Occurrence and density of Pacific saury *Cololabis saira* larvae and juveniles in relation to environmental factors during the winter spawning season in the Kuroshio Current system. Fish. Oceanogr. 23: 304–321, doi:10.1111/fog.12065

Takasuka, A., Oozeki, Y., and Aoki, I. 2007. Optimal growth temperature hypothesis, Why do anchovy flourish and sardine collapse or vice versa under the same ocean regime? Can. J. Fish. Aquat. Sci. 64: 768–776, doi:10.1139/f07-052

Takasuka, A., Oozeki, Y., and Kubota, H. 2008b. Multi-species regime shifts reflected in spawning temperature optima of small pelagic fish in the western North Pacific. Mar. Ecol. Prog. Ser. 360: 211–217, doi:10.3354/meps07407

Takasuka, A., Oozeki, Y., Kubota, H., and Lluch-Cota, S.E. 2008c. Contrasting spawning temperature optima, Why are anchovy and sardine regime shifts synchronous across the North Pacific? Prog. Oceanogr. 77: 225–232. doi: 10.1016/J.POCEAN.2008.03.008

Takasuka, A., Sakai, A., and Aoki, I. 2017. Dynamics of growth-based survival mechanisms in Japanese anchovy (*Engraulis japonicas*) larvae. Can. J. Fish. Aquat. Sci. 74: 812–823, doi:10.1139/cjfas-2016-0120

Tanaka, H., Sassa, C., Ohshimo, S., and Aoki, I. 2013. Feeding ecology of two lanternfishes *Diaphus garmani* and *Diaphus chrysorhynchus*. J. Fish Biol. 82: 1011–1031, doi:10.1111/jfb.12051

Tanimoto, Y., Kanenari, T., Tokinaga, H., and Xie, S.P. 2011. Sea level pressure minimum along the Kuroshio and its extension. J. Clim. 24: 4419–4434, doi: 10.1175/2011JCLI4062.1

Tanimoto, Y., Xie, S.-P., Kai, K., Okajima, H., Tokinaga, H., Murayama, T., Nonaka, M. and Nakamura, H. 2009. Observations of marine atmospheric boundary layer

transitions across the summer Kuroshio Extension. J. Clim. 22: 1360–1374, doi:10.1175/2008JCLI2420.1

Tokinaga, H., Tanimoto, Y., Xie, S.-P., Sampe, T., Tomita, H., and Ichikawa, H. 2009. Ocean frontal effects on the vertical development of clouds over the western North Pacific: In situ and satellite observations. J. Clim. 22: 4241–4260, doi: 10.1175/2009JCLI2763.1

Tomita, H., Xie, S,-P., Tokinaga, H., and Kawai, Y. 2013. Cloud response to the meandering Kuroshio Extension front. J. Clim. 26: 9393–9398, doi: 10.1175/JCLI-D-13-00133.1

Tsujino, H., Nishikawa, S., Sakamoto, K., Usui, N., Nakano, H. and Yamanaka, G. 2013. Effects of large-scale wind on the Kuroshio path south of Japan in a 60-year historical OGCM simulation. Clim. Dyn. 41: 2287–2318. doi, 10.1007/s00382-012-1641-4

Usui, N., Tsujino, H., Nakano, H., and Matsumoto, S. 2013. Long-term variability of the Kuroshio path south of Japan. J. Oceanogr. 69: 647–670, doi: 10.1007/s10872-013-0197-1

Watanabe, H. and Kawaguchi, K. 2003. Decadal change in abundance of surface migratory myctophid fishes in the Kuroshio region from 1957 to 1994. Fish. Oceanogr. 12: 100–111, doi.org/10.1046/j.1365-2419.2003.00225.x

Watanabe, H., Kawaguchi, K., and Hayashi, A. 2002. Feeding habits of juvenile surface migratory myctophid fishes. family Myctophidae. in the Kuroshio region of the western North Pacific. Mar. Ecol. Prog. Ser. 236: 263–272, doi: 10.3354/meps236263

Watanabe, Y., Zenitani, H., and Kimura, R. 1996. Offshore expansion of spawning of the Japanese sardine, *Sardinops melanostictus* , and its implication for egg and larval survival. Can. J. Fish. Aquat. Sci. 53: 55–61, doi:10.1139/f95-153

Wu, L., Cai, W., Zhang, L., Nakamura, H., Timmermann, A., Joyce, T., McPhaden, M.J., Alexander, M., Qiu, B., Visbeck, M., Chang, P., and Giese, B. 2012. Enhanced warming over the global subtropical western boundary currents. Nat. Clim. Change 2: 161–166, doi:10.1038/nclimate1353

Xu, H., Tokinaga, H., and Xie S.-P. 2010. Atmospheric effects of the Kuroshio large meander during 2004–05. J. Clim. 23: 4704–4715, doi: 10.1175/2010JCLI3267.1

Yatsu, A. and Kaeriyama, M. 2005. Linkages between coastal and open-ocean habitats and dynamics of Japanese stocks of chum salmon and Japanese sardine.

Deep. Sea Res. II 52: 727–737, doi: 10.1016/J.DSR2.2004.12.019

Yoshida, A., Asuma, Y. 2004. Structures and environment of explosively developing extratropical cyclones in the northwestern Pacific region. Mon. Wea. Rev. 132: 1121–1142, doi: 10.1175/1520-0493(2004)132<1121,SAEOED>2.0.CO;2

Yoshiike, S. and Kawamura, R. 2009. Influence of wintertime large-scale circulation on the explosively developing cyclones over the western North Pacific and their downstream effects. J. Geophys. Res. 114: D13110, doi: 10.1029/2009JD011820